Phylogenomic Species Delimitation Dramatically Reduces Species Diversity in an Antarctic Adaptive Radiation

Elyse Parker[1,*], Alex Dornburg[2], Carl D. Struthers[3], Christopher D. Jones[4], and Thomas J. Near[1,5]

[1]*Department of Ecology & Evolutionary Biology, Yale University, P.O. Box 208106, New Haven, CT 06520, USA;* [2]*Department of Bioinformatics and Genomics, University of North Carolina, Charlotte, Charlotte, NC 28223, USA;* [3]*Museum of New Zealand Te Papa Tongarewa, Wellington, New Zealand;* [4]*Antarctic Ecosystem Research Division, NOAA Southwest Fisheries Science Center, La Jolla, CA 92037, USA; and* [5]*Peabody Museum of Natural History, Yale University, New Haven, CT 06520, USA*
*Correspondence to be sent to: Department of Ecology and Evolutionary Biology, Yale University, New Haven, CT 06520, USA;
E-mail: chantal.parker@yale.edu.*

Abstract.—Application of genetic data to species delimitation often builds confidence in delimitations previously hypothesized using morphological, ecological, and geographic data and frequently yields recognition of previously undescribed cryptic diversity. However, a recent critique of genomic data-based species delimitation approaches is that they have the potential to conflate population structure with species diversity, resulting in taxonomic oversplitting. The need for an integrative approach to species delimitation, in which molecular, morphological, ecological, and geographic lines of evidence are evaluated together, is becoming increasingly apparent. Here, we integrate phylogenetic, population genetic, and coalescent analyses of genome-wide sequence data with investigation of variation in multiple morphological traits to delimit species within the Antarctic barbeled plunderfishes (Artedidraconidae: *Pogonophryne*). *Pogonophryne* currently comprises 29 valid species, most of which are distinguished solely by variation in the ornamentation of the mental barbel that projects from the lower jaw, a structure previously shown to vary widely within a single species. However, our genomic and phenotypic analyses result in a dramatic reduction in the number of distinct species recognized within the clade, providing evidence to support the recognition of no more than six species. We propose to synonymize 24 of the currently recognized species with five species of *Pogonophryne*. We find genomic and phenotypic evidence for a new species of *Pogonophryne* from specimens collected in the Ross Sea. Our findings represent a rare example in which the application of molecular data provides evidence of taxonomic oversplitting on the basis of morphology, clearly demonstrating the utility of an integrative species delimitation framework.[ddRADseq; multispecies coalescent; Notothenioidei; SNPs; Southern Ocean.]

The 21st century has ushered in a species delimitation renaissance that is largely driven by advances in genomic-scale DNA sequencing technologies and theoretical advances such as the multispecies coalescent (MSC) (Degnan and Rosenberg 2009). The application of statistical species delimitation approaches to data sets comprising hundreds to thousands of genetic loci has yielded an unprecedented resolution of species boundaries, including lineages with relatively recent common ancestry, where processes such as incomplete lineage sorting and hybridization potentially hinder accurate delimitation of species (Wagner et al. 2013; Ješovnik et al. 2017; Musher and Cracraft 2018; Kornilios et al. 2020). However, genomic data also hold considerable power for the detection of fine-scale genetic structure within species, which can be difficult to distinguish from species-level divergences. Species delimitation approaches that rely on analyses of genomic data alone therefore run the risk of conflating population-level structure with species boundaries, which can potentially lead to inflated estimates of species diversity (Sukumaran and Knowles 2017; Chambers and Hillis 2020; Mason et al. 2020). As such, an increasingly adopted perspective on species delimitation calls for a more robust approach that integrates genomic analyses with multiple sources of information, such as morphology

and ecology (Rissler and Apodaca 2007; Edwards and Knowles 2014; Pante et al. 2015; Solís-Lemus et al. 2015).

Integrative species delimitation studies are of particular importance for understanding patterns of Antarctic marine biodiversity. Recognition of the incredible species diversity that resides in the Southern Ocean of Antarctica has accrued over the last decade (Chown et al. 2015) and continued exploration suggests a dramatic underestimate of Antarctic species richness (Brandt et al. 2007). However, many Antarctic species are delimited solely on the basis of a few morphological characters (e.g., Bernardi and Goswami 1997; La Mesa et al. 2002; Lautredou et al. 2010; Nikolaeva and Balushkin 2019). This weight placed on a few characters as evidence of species boundaries situates Antarctic science in a precarious position. Chance trait convergence may undermine analysis results based on the assumption of accurate species delimitation. Furthermore, it is becoming clear that some traits fail to diagnose morphologically similar but genetically distinct species of vertebrate and nonvertebrate animals (Wilson et al. 2009; Brasier et al. 2016; Dornburg et al. 2016b). Therefore, testing the credibility of currently recognized Antarctic species boundaries is a fundamental prerequisite in the investigation of the mechanisms responsible for generating the unique biodiversity of the Southern Ocean.

58

Among Antarctic vertebrates, cryonotothenioids (*sensu* Near et al. 2015) dominate the vertebrate fauna of near-shore Antarctic marine habitats, comprising the majority of the biomass, abundance, and species diversity of fishes (Eastman 2005; Near et al. 2012; Matschiner et al. 2015). Although one of the few examples of vertebrate adaptive radiation in marine habitats, macroevolutionary analyses of the cryonotothenioid radiation are challenged by the uncertainty of the number of species in the clade (Lautredou et al. 2012; Dornburg et al. 2016b). The description of new species typically builds confidence in the assessment of lineage diversity, but since the late 1980s most new species of cryonotothenioids are described on the basis of a small number of specimens with morphological delimitations that appear atypical relative to other contemporary descriptions of teleost fish species (e.g., Balushkin and Spodareva 2015; Eakin et al. 2015). The problematic nature of recent notothenioid species descriptions is apparent in the plunderfishes (Artedidraconidae), a clade that is largely endemic to the high Antarctic latitudes and was highlighted as the most rapidly diversifying of all cryonotothenioid subclades (Near et al. 2012).

Within Artedidraconidae, presumptive new species of *Pogonophryne* Regan 1914 are described at a rate that far exceeds all other notothenioid lineages. *Pogonophryne* currently comprises 29 valid species, of which 13 were described since the start of the 21st century (Eschmeyer and Fricke 2020). However, these recent descriptions depart from common conventions of species descriptions that make use of comparative material to assess the reliability of presumed diagnostic traits in the face of population-level variation. Among the newest species of *Pogonophryne*, six are based on a single specimen (Eakin and Balushkin 2000; Eakin et al. 2008; Balushkin and Spodareva 2013b; Spodareva and Balushkin 2014; Balushkin and Spodareva 2015), four are based on two specimens (Eakin et al. 2009; Balushkin et al. 2011; Balushkin 2014; Balushkin and Korolkova 2013; Balushkin and Spodareva 2013a), and no species described since 2000 is based on more than four specimens (Balushkin and Spodareva 2013c; Shandikov and Eakin 2013; Shandikov et al. 2013). Variation in the morphology of the mental barbel represents the most important diagnostic trait for all of the 23 species of *Pogonophryne* described since *Pogonophryne albipinna* Eakin 1981. Despite the heavy reliance on barbel morphology in describing species of *Pogonophryne*, the mental barbel in *Pogonophryne scotti* Regan 1914 exhibits extensive intraspecific embellishment, with the terminal expansion of the barbel varying from short and tapered to long and covered in many different kinds of folds and papillae (Eakin et al. 2001). Given the extensive intraspecific variation in mental barbel morphology coupled with a lack of distinction among species in other meristic and morphometric traits, the credibility of *Pogonophryne* species delimitations based on barbel morphology alone is questionable.

The first major study of interspecific relationships within *Pogonophryne* divided all known species into two groups based on differences in mottling patterns: the "dorsally unspotted group," comprising three species, and the "dorsally spotted group," which included four species (Eakin 1977). A third group, known as the "unspotted" group, was described by Eakin (1981) to accommodate the discovery of two *Pogonophryne* species that lack dark markings on the body and head. Most recently, Balushkin and Eakin (1998) expanded upon the species group classification criteria to include variation in meristic traits and craniofacial features in addition to spotting patterns. Using these new diagnostic characters, they proposed classifying *Pogonophryne* species into the five species groups that are currently recognized (Balushkin and Eakin 1998). The "dorsally unspotted group" is now considered to comprise a single species, *P. scotti*. Characteristic of the *P. scotti* group is the absence of dark blotches on the dorsal surface of the head, as well as a relatively small number of vertebrae (35–37) and second dorsal-fin rays (24–26; Balushkin and Eakin 1998; Eastman and Eakin 2000). The six species of the *P. albipinna* group (referred to as the "unspotted" group) are altogether lacking in dark markings along with the head and body and are distinguished by a relatively high number of vertebrae (37; Eakin 1981; Eakin et al. 2009). The remaining three groups represent the "spotted groups." The *Pogonophryne mentella* group is the largest, with 15 species, all of which are distinguished by rounded mottling on the dorsal and lateral surfaces of the head and a protruding lower jaw. The diagnostic character of the *Pogonophryne marmorata* group, with five species, is a marked indentation in the anterior part of the eye socket. The two species making up the *Pogonophryne barsukovi* group are identified by a pronounced slope in the snout and dark speckling on the head (Balushkin and Eakin 1998; Eastman and Eakin 2000).

Species within each of these groups are delimited on the basis of the length of the mental barbel and morphology of the barbel terminal expansion. While previous phylogenetic inferences and assessments of genetic divergence using mitochondrial DNA sequences support the monophyly of the five species groups, species within the *P. albipinna* and *P. mentella* groups are paraphyletic (Eakin et al. 2009). In addition, the maximum mtDNA pairwise genetic divergence among any species of *Pogonophryne* was shallow at 1.4%, and haplotypes were shared among species within species groups (Eakin et al. 2009; Smith et al. 2012). Overall, these findings suggest strong support for the genetic distinctiveness of each of the five currently recognized species groups but do not find support for genetic differentiation among traditionally recognized species within each group. The extensive intraspecific variation in the mental barbel, which is the primary structure used to delimit species, coupled with limited genetic differentiation and lack of reciprocal monophyly among described species begs the question: how many species of *Pogonophryne* are there?

Here, we test species delimitations and investigate phylogenetic relationships of *Pogonophryne* using a series of analyses based on more than 100,000 loci captured using restriction site-associated DNA sequencing from 218 specimens sampled from 18 of the 29 currently recognized species of *Pogonophryne*. Phylogenomic species delimitations were assessed with analyses of morphometric and meristic traits traditionally used to discover and describe species of teleost fishes. The evidence from phylogenomic and phenotypic analyses supports a dramatic reduction of the number of distinct species of *Pogonophryne*, suggesting a sustained taxonomic oversplitting in this lineage of cryonotothenioids.

MATERIALS AND METHODS

Taxon Sampling and ddRAD Sequencing

We used double-digest restriction site-associated DNA sequencing (ddRADseq) to collect genome-wide sequence data for *Pogonophryne* specimens following a protocol modified from Peterson et al. (2012). Taxon sampling included a total of 228 individuals representing 18 of the 29 currently recognized *Pogonophryne* species and all five species groups in addition to eight artedidraconid species included as outgroup taxa (Supplementary Table S1 available on Dryad at http://dx.doi.org/10.5061/dryad.4f4qrfjc3). Many species of *Pogonophryne* are known only from holotype or type series, thus tissue samples are not available for 11 currently recognized species. Specimens were collected from locations across a nearly circum-Antarctic distribution between 2001 and 2019 (Fig. 1; Supplementary Table S1 and Fig. S1 available on Dryad). Antarctic Marine Living Resources (AMLR) cruises conducted in the austral summers of 2001, 2003, 2006, and 2009 yielded specimens from the Antarctic Peninsula, South Shetland Islands, Elephant Island, and the South Orkney Islands. Benthic trawls were used to collect all specimens, and muscle tissue samples were taken and stored in 95% ethanol. Tissue samples and their associated voucher specimens were provided to the Yale Peabody Museum of Natural History. Loans provided by the Museum of New Zealand Te Papa Tongarewa yielded tissue samples from the Ross Sea and Wilkes Land, and loans provided by the University of Padova, Padova, Italy furnished tissue samples from the Weddell Sea (Supplementary Table S1 and Fig. S1 available on Dryad).

Whole genomic DNA was extracted from tissues using the Qiagen DNeasy Kit (Qiagen Inc., Valencia, CA, USA) following manufacturer protocol. Prior to library preparation, DNA concentration was quantified using a Qubit fluorometer (Thermo Fisher Scientific) as well as through visual examination using a 1% agarose gel. Ethanol precipitation of DNA was performed to concentrate whole genomic DNA and to remove contaminants such as salts which could interfere with enzymatic digestion or Qubit quantifications (Nakayama et al. 2016). Library preparation of ddRADseq loci began with

double digestion of ~200 ng of DNA from each sample using the PstI and MspI restriction enzymes for 16 h. After confirming digestion of all samples using a 1% agarose gel, common MspI adapters and sample-specific barcoded PstI adapters were ligated to the digested fragments. We then combined equimolar amounts of each sample into pools containing four unique barcoded samples each and cleaned each pool using the QIAquick Purification Kit following manufacturer protocol. The cleaned libraries were then amplified using polymerase chain reaction (PCR) in $50\mu L$ reactions consisting of $10\mu L 5\times$ Phusion Buffer HF, $1\mu L$ 10mM DNTPs, $1.5\mu L$ DMSO, $1\mu L$ each of $10\mu M$ PstI and $10\mu M$ MspI primers, $1\mu L$ Phusion High Fidelity DNA Polymerase, $6\mu L$ DNA library template, and 29μ LDNase-free water. Following PCR, libraries were again pooled, with each pool containing 24 unique barcoded samples, and these pools were cleaned using the QIAquick Purification Kit. After using an Agilent 2100 Bioanalyzer Instrument to assess the size distribution, quantity, and purity of the DNA in each of our indexed libraries, we pooled equimolar amounts of each of our libraries into three 95-sample multiplexed libraries (one library contained 56 samples for another project). The pooled libraries were size-selected for fragments between 300 and 500 bp on a 2% agarose gel using the Blue Pippin DNA Size Selection System (Sage Science) according to manufacturer protocol. Size-selected libraries were again checked for appropriate fragment length distribution and DNA quality using the Agilent 2100 Bioanalyzer, and a Qubit fluorometer was used to quantify DNA concentrations. Each of the final ddRAD libraries was then sequenced on an Illumina HiSeq 2000 using single-end sequencing at the University of Oregon GC3F facility (https://gc3f.uoregon.edu/). In order to mitigate the potential for the conflation of biological signals with batch effects introduced during library preparation or sequencing, we randomly distributed samples representing each of the five traditionally recognized species groups across each of the three ddRAD libraries.

Bioinformatic processing of the sequenced ddRAD libraries was performed using the software ipyrad v0.9.50 (http://github.com/dereneaton/ipyrad/). First, raw sequence reads were demultiplexed using sample-specific barcodes, and reads with more than five bases with a phred Q-score <20 were excluded from downstream processing. Illumina adapters were filtered out using the software cutadapt (implemented within the ipyrad pipeline by setting the *filter_adapters* parameter to 2). Next, the vsearch tool was used for *de novo* clustering of reads within samples based on a quantitatively optimized sequence similarity threshold, and the resulting clusters were aligned using the MUSCLE algorithm (Edgar 2004). Clusters with a sequencing depth of less than six reads were excluded from downstream processing, and consensus allele sequences estimated from clustered reads were discarded if they contained more than 5% ambiguous sites ("N"s) or if they contained more than 5% heterozygous bases. The remaining consensus sequences were then clustered as homologous
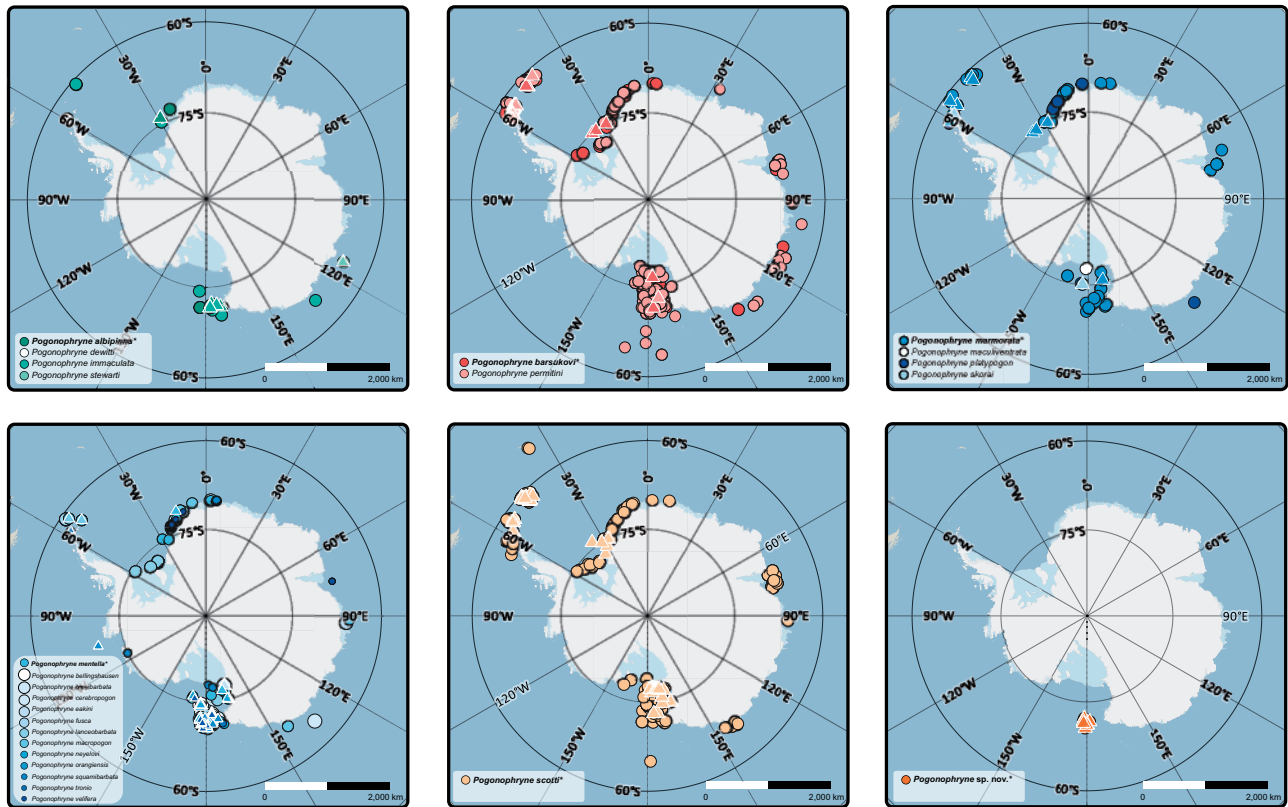
FIGURE 1. Distribution of *Pogonophryne* species visualized using collection records compiled from specimens used in this study (Supplementary Tables S1 and S4 available on Dryad; Supplementary Fig. S1a,b available on Dryad); from GBIF (https://doi.org/10.15468/dl.gp755t); from the Museum of New Zealand Te Papa Tongarewa; and from Duhamel et al. (2014). To facilitate visualization, separate maps were generated for each of the five traditionally defined species groups and for a putatively new lineage identified in this study, *Pogonophryne* sp. nov. Circles represent all collection records, and triangles represent collection records only for samples used in genomic analyses in this study. All points are colored according to species. In each map legend, species names that are bolded and asterisked represent the nominal species of each species group. (For interpretation of the references to color in this figure, the reader is referred to the web version of this article.)

loci across samples using the optimal sequence similarity threshold, and loci shared by fewer than four individuals were excluded from the final data set.

In order to identify the optimal sequence similarity threshold for clustering reads within samples (Step 3 of ipyrad) and between samples (Step 6 of ipyrad), we generated a set of ddRAD assemblies under threshold values ranging from 88% to 95% and calculated four metrics for each assembly: i) per-individual percent heterozygosity; ii) total number of variable sites (SNPs); iii) cumulative variance explained by the first eight principal components (PCs) retained from a principal components analysis (PCA) of the genetic data; and iv) Pearson's correlation coefficient between pairwise genetic dissimilarity and data missingness (McCartney-Melstad et al. 2019; Supplementary Fig. S2 available on Dryad). We used scripts available from McCartney-Melstad et al. (2019) to calculate metrics 3 and 4 and to generate heatmaps visualizing pairwise data missingness (Xiuwen et al. 2012; Galili 2015; Mastretta-Yanes et al. 2015; Kolde 2018; Potter 2018). Metrics 1 and 3 identify a sequence similarity threshold of 88% as optimal for our data set, with per-individual heterozygosity

and cumulative variance explained by the first 8 PCs both maximized at an 88% threshold (Supplementary Fig. S2a and c available on Dryad). On the other hand, metric 2 identifies a sequence similarity threshold of 95% as optimal, with the total number of SNPs in the assembly maximized at this value (Supplementary Fig. S2b available on Dryad). Finally, metric 4 identifies an optimal clustering threshold at 93%, as this is the value at which the correlation between pairwise genetic distance and pairwise missingness begins to sharply increase (Supplementary Fig. S2d available on Dryad). Given the apparent lack of consensus across our calculated metrics regarding an optimal sequence similarity threshold, we conducted preliminary phylogenetic analyses (using IQ-TREE and tetrad, see below for detailed methods) based on data sets derived from assemblies generated under the minimum (88%) and maximum (95%) threshold values we tested. These analyses yielded concordant results regarding phylogenetic relationships among sampled individuals (Supplementary Fig. S3a–g available on Dryad). Similarly, genotypic clustering analyses (using STRUCTURE and DAPC, see below for detailed methods) based on data sets generated under

88% and 95% clustering thresholds yielded concordant results regarding the identification of genotypic clusters and assignment of individuals to these clusters (Supplementary Figs. S4a–h and S5 available on Dryad). Thus, the results of phylogenetic and genotypic clustering analyses appear robust to our choice of clustering threshold. Given this, we selected an optimal clustering threshold of 88% for all downstream processing, as this was identified as the "optimal" value by two out of the four calculated metrics. This choice of clustering threshold also satisfies the recommendation of O'Leary et al. (2018) to favor clustering thresholds that reduce the possibility of oversplitting naturally occurring allelic variation into separate loci.

The ddRAD assembly generated under the 88% sequence similarity threshold included 262,359 loci shared across at least four individuals (hereafter referred to as the "min4" data set). We additionally generated a set of assemblies including varying amounts of missing data. Previous work has demonstrated that stricter thresholds on the amount of missing data may produce data sets that exclude loci with the highest mutation rates. As a consequence, data sets with lower proportions of missing data may also include fewer variable sites, which could have an impact on the patterns of genetic variation inferred from phylogenetic, genotypic clustering, and genomic species delimitation analyses (Huang and Knowles 2016). In order to test the effect of missing data on downstream analyses, we constructed the following three assemblies that respectively reflect thresholds of 75%, 50%, and 25% missing data: i) a data set including only loci shared across at least 58 individuals (min58; 102,396 loci); ii) a data set including only loci shared across at least 116 individuals (min116; 62,029 loci); and iii) a data set including only loci shared across at least 174 individuals (min174; 28,272 loci) (Supplementary Table S2 available on Dryad). While each of these data sets differs in the number of loci retained and their proportions of missing data, they each include all 228 individuals sampled for genomic analyses.

Phylogenomic Analyses

The phylogenetic relationships among species of *Pogonophryne* were inferred using both concatenation-based and MSC-based methods. Under both analytical frameworks, we analyzed each of the min58, min116, and min174 data sets to evaluate the impact of different levels of missing data on the phylogenetic inferences. We used the IQ-TREE software package (Nguyen et al. 2015) to infer a maximum likelihood (ML) phylogeny for *Pogonophryne* based on matrices of concatenated sequences from loci recovered in each of the min58, min116, and min174 data sets. Prior to phylogenetic analysis, we identified the best-fit nucleotide substitution model for each data set using ModelFinder (Kalyaanamoorthy et al. 2017). Node support was assessed using an ultrafast bootstrap approximation

(UFboot) with 1000 replicates (Minh et al. 2013; Hoang et al. 2018). Our species tree analyses were conducted using tetrad, an implementation of the program SVD-quartets (Chifman and Kubatko 2014) in ipyrad, to infer a species tree under the MSC from an alignment of unlinked single nucleotide polymorphisms (SNPs). Over the course of the analyses, SNP alignments were subsampled such that, for each bootstrap replicate, a single SNP was randomly selected from each locus for each quartet inference in the analysis. We inferred 4,050,786 random quartets, and the individual quartet trees were joined into a single supertree using the wQMC algorithm (Snir and Rao 2012). Nonparametric bootstrapping was used to assess node support, and a 50% majority-rule consensus tree was generated from 1000 bootstrap replicates.

Population Structure and Differentiation

We used two different approaches to assign the *Pogonophryne* individuals sampled in this study to genetic clusters without *a priori* information about genetic structure or individual assignment to genetic groups. First, a Bayesian clustering algorithm implemented in the program STRUCTURE v2.3.4 (Pritchard et al. 2000) was used to infer the number of genetic clusters within *Pogonophryne* and probabilistically assign individuals in our data set to each of the identified clusters (or to multiple clusters if individuals are admixed). We built a separate assembly of ddRADseq loci excluding all outgroup taxa from our data set and including only loci shared across at least 195 of the remaining 218 individuals ("noOut_min195"; 11% missing data; Supplementary Table S2 available on Dryad). This filtering scheme resulted in the retention of 1317 loci, from which we randomly extracted a total of 1166 unlinked SNPs for analysis. Our analysis tested clustering scenarios ranging from 2 to 29 groups (K = 2–29), where the upper bound of 29 clusters represents the total number of *Pogonophryne* species recognized by the current taxonomy. We ran 10 replicate analyses for each value of K for 1,000,000 generations each and discarded the first 100,000 generations as burn-in. For all analyses, we applied a model of correlated allele frequencies, and we assume a model with admixture. However, because the correlated allele model has the potential to overestimate the optimal number of clusters (Falush et al. 2007), we repeated all analyses under an uncorrelated allele model to assess whether the different models impacted our interpretations of populations structure. The convergence of replicate runs was determined by evaluating the variance of the alpha parameter and log-likelihood scores. The optimal number of clusters was estimated using the method of Evanno et al. (2005) implemented in Structure Harvester as well as by evaluating the log probability of the data (log $P(X|K)$). Results of replicate runs were summarized and visualized using CLUMPP v1.1.2 (Jakobsson and Rosenberg 2007) and distruct v1.1 (Rosenberg 2004). In

order to evaluate further substructure in our data set, we performed a set of nested STRUCTURE analyses within clusters identified by analysis of the full *Pogonophryne* data set (Coulon et al. 2008). We used ipyrad to construct separate ddRAD assemblies for each of the clusters identified by our full STRUCTURE analysis in order to maximize the loci available for the hierarchical analyses (following Devitt et al. 2019). For each of these data subsets, we only included loci shared across ~90% of the individuals in order to minimize the proportion of missing data included in each data set and to ensure that approximately 1000 unlinked SNPs were retained in each data set (Supplementary Table S2 available on Dryad). For each of our hierarchical STRUCTURE analyses, all parameter specifications were the same as those described in the above paragraph.

In addition to the Bayesian approach used by STRUCTURE, we implemented a discriminant analysis of principal components (DAPC) in the R package adegenet (Jombart and Ahmed 2011) to identify the number of groups in our *Pogonophryne* data set that maximizes the genetic difference between groups while minimizing the differentiation of individuals within groups. We used ipyrad to build different assemblies of ddRAD loci that excluded all outgroup taxa, and that included varying levels of missing data for each assembly. This yielded four different data sets for analyses, each of which included a total of 218 individuals i) a data set including only loci shared across at least 55 individuals ("noOut_min55"; 90,459 unlinked SNPs and 75% missing data); ii) a data set including only loci shared across at least 110 individuals ("noOut_min110"; 56,499 unlinked SNPs and 50% missing data); iii) a data set including only loci shared across at least 165 individuals ("noOut_min165"; 26,271 unlinked SNPs and 25% missing data); and iv) a data set including only loci shared across at least 197 individuals ("noOut_min197"; 624 unlinked SNPs and 90% missing data) (Supplementary Table S2 available on Dryad). We first transformed each data set using PCA and then used a *k*-means clustering algorithm to identify the optimal number of clusters (*k*) in our data set by sequentially increasing the value of *k* between 1 and 29. We identified the optimal clustering scenario as the value of *k* that minimized the Bayesian Information Criterion (BIC). We then performed a Discriminant Analysis on the optimal number of PCs selected using cross-validation in order to identify the discriminant functions that best described the extent of genetic variation among identified clusters. Results of DAPC were visualized using the "scatter" and "compoplot" functions within adegenet (Jombart and Ahmed 2011).

We calculated a population genetic statistic and a measure of genetic divergence to evaluate genetic differentiation between traditionally recognized species groups as well as between traditionally recognized species within each group (with the exception of the *P. scotti* species "group," which is monotypic). For the *P. barsukovi* and *P. scotti* species groups, for which we have widespread geographic sampling (Supplementary Fig. S1 available on Dryad), we additionally assigned individuals to populations according to sampling locality and evaluated genetic differentiation between these geographically delimited groups. Pairwise F_{ST} statistics were calculated using the weighted Weir and Cockerham (1984) estimator implemented in VCFtools (Danecek et al. 2011). We also calculated Nei's genetic distance metric (D_{Nei}) using the function "nei.dist" implemented in the R package poppr v.2.91 (Kamvar et al. 2014, 2015). All population differentiation statistics were calculated using the same "noOut_min195" data set analyzed using STRUCTURE.

Species Delimitation

We used BPP v 4.1 (Yang and Rannala 2010, 2014) to test among candidate species delimitation hypotheses for *Pogonophryne* using a fixed guide tree (Analysis A10). This program implements Bayesian reversible-jump MCMC (rjMCMC) inference of the posterior probabilities of alternative species delimitation models given a multiple sequence alignment of phased allele data and a guide species tree. In order to improve the mixing of the rjMCMC algorithm, taxonomic sampling in our data set was reduced to include 21 *Pogonophryne* individuals representing a total of 19 candidate species. This species delimitation hypothesis reflects the number of traditionally defined *Pogonophryne* species represented in our ddRAD data set (18 species) in addition to a putatively new lineage hereafter referred to as *Pogonophryne* sp. nov. All candidate species were represented by a single individual except for *P. scotti* and *Pogonophryne* sp. nov., which were each represented by two individuals. We used ipyrad to build a separate ddRAD assembly for these 21 individuals in order to maximize the number of loci shared across sampled individuals. We estimated a guide tree for these individuals from a tetrad analysis of unliked SNPs randomly sampled from 964 loci shared across all 21 individuals. In order to reduce the computational burden of the species delimitation analysis, we restricted our BPP analyses to 100 randomly selected loci that were shared across all individuals in our data set. Our tests considered all possible models delimiting between one and 21 species (where each individual is treated as representing a unique species), which allowed us to test the validity of the 19 candidate species while also enabling BPP to explore different species delimitation models and different assignments of individuals to species (Olave et al. 2014).

Following the suggestions of Yang (2015), we implemented two different rjMCMC algorithms for guided species delimitation (A10) analyses in BPP i) Algorithm 0, with $\varepsilon = 2$; and ii) Algorithm 1, with $\alpha = 2$ and $m = 1$. For each algorithm, we tested the influence of prior specifications on our results by running analyses under all four possible combinations of two different priors on population size (θ) ($\theta \sim$ IG [3,0.2] and $\theta \sim$ IG [3,0.002]) and on divergence time (τ) ($\tau \sim$ IG [3,0.2] and $\tau \sim$ IG [3,0.002]). We conducted three replicate runs of each analysis under every possible combination of priors and species delimitation algorithms. We conducted

sampling every five generations for a total of 5,000,000 samples, discarding the first 4000 samples as burn-in. We checked for convergence of replicate runs by visually evaluating the consistency of the posterior distributions of the model parameters and log-likelihoods, and we checked that a different starting delimitation was used for each replicate run.

Divergence Time Estimation

We used the approach employed by Stange et al. (2018) to estimate divergence times among candidate species of *Pogonophryne* using the SNAPP v1.5.0 package (Bryant et al. 2012) of BEAST v2.6.0 (Bouckaert et al. 2019). Because of the prohibitively long run times that would result from the analysis of the full data set, we analyzed a matrix of 1009 unlinked biallelic SNPs for a subset of 20 individuals representing each of the six candidate *Pogonophryne* species identified by phylogenetic, population structure, and coalescent analyses. Our subsampling strategy included 3–4 individuals per species and sought to maximize the geographic distribution of individuals representing each of the six delimited species while also minimizing the amount of missing data for each individual. A separate ddRAD assembly was constructed for the 20-individual subset in order to maximize the number of loci shared across the included specimens. After retaining only those loci shared across at least 19 of the 20 samples, our data set included a total of 4393 loci. We then used ipyrad to randomly select a single SNP per locus and used the "phrynomics" R package (https://github.com/bbanbury/phrynomics) to remove all invariant sites and all nonbinary sites, resulting in a final data matrix consisting of 1009 unlinked SNPS.

Given the lack of known cryonotothenioid fossils, the root node representing the most recent common ancestor (MRCA) of *Pogonophryne* was calibrated using a normal distribution with a mean of 1.1 Ma and a standard deviation of 0.23 Myr based on the age estimate derived from a previous study (Near et al. 2012). In order to improve the mixing of the MCMC, we enforced monophyly of each of the six delimited *Pogonophryne* species based on the consistently strong bootstrap support for each of these clades across all of our other phylogenetic analyses. We conducted four replicate runs of the analysis for 10,000,000 MCMC iterations each and discarded the first 10% of iterations as burn-in. The software Tracer v.1.7 (Rambaut et al. 2014) was used to evaluate stationarity of parameter estimates in each analysis and convergence of parameter estimates across replicate runs, where ESS values >200 were interpreted as support for stationarity. The posterior tree distributions from the four replicates were then combined and used to estimate a maximum clade credibility tree using TreeAnnotator v2.6.0.

Morphology

In order to evaluate patterns of phenotypic variation within *Pogonophryne*, we compiled data on 26 linear morphometric and five meristic traits for 16 traditionally delimited species that represent all five traditionally defined species groups (Supplementary Table S3 available on Dryad). Counts and measurements were obtained from both published manuscripts (Eakin 1981; Eakin and Kock 1984; Eakin 1988a, 1988b; Balushkin 1991; Eakin and Eastman 1998; Balushkin 1999) and data used in several species descriptions provided by Drs Joseph T. Eastman and Richard R. Eakin (pers. comm.). The morphological data set included 256 adult specimens spanning a circum-Antarctic geographic distribution (Supplementary Table S4 available on Dryad). These specimens included a total of 38 individuals also represented in the ddRADseq data set. Institutional museum collection acronyms follow Sabaj (2016) with the exceptions of YFTC (Yale Peabody Museum of Natural History Tissue Collection) and UMDC (Ira D. Darling Centre, University of Maine). In addition, we collected data for the five meristic traits and 26 linear measurements as outlined in Balushkin and Eakin (1998) and Eakin and Eastman (1998) for four *Pogonophryne* specimens identified from genomic analyses as representing a potentially new species. All measurements were taken to the nearest 0.01 mm using needlepoint digital calipers. We analyzed the 26 linear morphometric characters using PCA to visualize patterns of disparity along axes of body shape variation. Prior to analysis, all morphometric traits were $\log_{10}$- transformed, and we controlled for potential correlation between body size and each of the morphometric trait variables by using the residuals from a linear regression of each log-transformed trait against the log standard length (SL). Regression analyses were conducted separately for each species group to account for potential heterogeneity in allometric scaling. The "prcomp" R function was then used to perform PCA on the residuals in order to visualize the extent of overlap along major axes of body shape variation among *Pogonophryne* species groups, as well as among species within species groups. Additionally, in order to account for potential sexual dimorphism in body shape, we applied the same regression-based control for the effects of body size independently for males and for females sampled for each traditionally recognized species group. We then conducted a second set of PCAs focused on evaluating body shape differences between males and females within each of the *P. barsukovi*, *P. scotti*, *P. mentella*, and *P. marmorata* species groups (the *P. albipinna* group could not be evaluated for sex-related differences in body shape because only two female individuals were included in our data set). In order to visualize separation among *Pogonophryne* species in meristic characters, we first conducted a PCA of the $\log_{10}$-transformed meristic data using the "prcomp" function in R. The Kruskal–Wallis and pairwise rank-sum Wilcoxon tests were then used to evaluate the significance of differences of the mean meristic trait values across *Pogonophryne* species groups as well as across species within each group.

Preliminary examination of radiographs revealed that, for the four specimens representing the potentially new species, the length of the lower jaw in proportion to SL

appeared longer than for other species of *Pogonophryne*. However, lower jaw length was not included as a character in the historical linear morphometric data we compiled. Thus, using digital calipers, we measured the standard length (SL), head length (HL), and length of the lower jaw (LJL) for 54 specimens representing 9 *Pogonophryne* species and all 5 traditionally described species groups in addition to the 4 specimens representing the putatively new species (Supplementary Table S4 available on Dryad). We calculated the ratios of the LJL to SL as well as LJL to HL and used a nonparametric Kruskal–Wallis test and a pairwise rank sum Wilcoxon test to evaluate the significance of differences in the mean ratios across the traditionally defined species groups and the potentially new species.

We evaluated variation in mental barbel shape and ornamentation for the *P. barsukovi* and *P. marmorata* species groups by examining and scoring 56 of the 63 specimens of *P. barsukovi* and *Pogonophryne permitini* and 4 of the 13 specimens of *P. marmorata* and *Pogonophryne skorai* sampled in our genomic analyses. Specimens were assigned to one of two barbel types based on the shape and dermal projections of the terminal expansion, that is, with a terminal expansion representing that described for *P. barsukovi* or for *P. permitini*, following the descriptions provided in Andriashev (1967) and Eakin (1990).

RESULTS

Phylogenomic Analyses

Inferred phylogenetic trees were highly concordant across ML-based and MSC-based analyses of each of our ddRAD data sets in strongly supporting reciprocal monophyly of each of the five *Pogonophryne* species groups and a newly discovered *Pogonophryne* sp. nov. lineage (bootstrap support $\geq$ 99 in all phylogenies; Fig. 2 and Supplementary Fig. S3 available on Dryad). The relationships among the six major lineages were consistent and strongly supported in both the ML- and MSC-based phylogenetic analyses, regardless of variation in the proportion of missing data (bootstrap support $\geq$ 99 in all phylogenies; Fig. 2 and Supplementary Fig. S3 available on Dryad).

Within each of the six major lineages, the monophyly of traditionally delimited species received little-to-no support across phylogenetic analyses. Specifically, within the *P. barsukovi*, *P. marmorata*, and *P. mentella* groups, individuals assigned to the same species based on morphology were never resolved as monophyletic groups, regardless of the analytical framework applied, the number of loci analyzed, or the proportion of missing data. Within the *P. albipinna* clade, the monophyly of each of the morphological species is inconsistently resolved, with *Pogonophryne immaculata* resolved as monophyletic across three IQ-TREE analyses and one tetrad analysis with highly variable support (bootstrap support = 4–100) and the monophyly of *Pogonophryne stewarti* only weakly supported by the results of tetrad (bootstrap

support = 17–23) (Supplementary Fig. S3 available on Dryad).

Population Structure

Results of STRUCTURE analyses identified six (K = 6) discrete clusters within *Pogonophryne* corresponding to distinctions among each of the five *Pogonophryne* species groups and the new lineage, *Pogonophryne* sp. nov., as resolved in the phylogenetic analyses (Fig. 3b). This sixth cluster, *Pogonophryne* sp. nov., comprises seven individuals: four individuals each identified from morphology to three different species within the *P. mentella* species group; one identified morphologically as *P. marmorata*; one as *P. permitini* (belonging to the *P. barsukovi* species group); and one individual identified by the collector as potentially representing a new *Pogonophryne* species. Nearly all other sampled individuals were assigned to each of the *P. scotti*, *P. marmorata*, *P. mentella*, *P. barsukovi*, and *Pogonophryne* sp. nov. clusters with high posterior probability (PP $\geq$ 0.95). Only one individual initially identified as *Pogonophryne neyelovi* (NMNZ P.049757) from the Ross Sea appears to be a hybrid between the newly discovered *Pogonophryne* sp. nov. and *P. mentella* (Fig. 3b). In the analysis of the full data set, all samples morphologically identified to the *P. albipinna* species group exhibit admixed ancestry from each of the *P. mentella* and *P. marmorata* clusters as well as from a third unique cluster (the green cluster) which we refer to as the *P. albipinna* cluster. However, subsequent analyses including only individuals assigned to each of these three clusters resulted in the identification of three discrete entities corresponding to clear distinctions among the *P. albipinna*, *P. mentella*, and *P. marmorata* species groups with almost no evidence of admixture among them (Fig. 3b). A single individual from the Ross Sea assigned to the *P. albipinna* group (NMNZ P.046208) additionally exhibits evidence of admixed ancestry with the *P. scotti* cluster (Fig. 3b) in analysis of the full data set, suggesting the possibility of at least some gene exchange among these lineages. Additional STRUCTURE analyses within each of the *P. barsukovi*, *P. scotti*, and *P. mentella* clusters found no pattern of substructure, with almost all individuals in each group assigned with high confidence (PP $\geq$ 0.95) to a single genetic cluster across a range of *K* values (Fig. 3b). These results remained consistent regardless of whether a correlated or uncorrelated model of allele frequencies was used, and we therefore present only the results of analyses under the model of correlated frequencies (Fig. 3b). Complementing these findings, the *k*-means clustering approach implemented in adegenet also consistently supported recognition of six population clusters reflecting distinctions among each of the five species groups and the newly discovered *Pogonophryne* sp. nov. cluster. Furthermore, regardless of the number of SNPs analyzed or the amount of missing data retained in each data set, individuals were assigned with high confidence to the same clusters as in the STRUCTURE analyses based on the retained discriminant functions
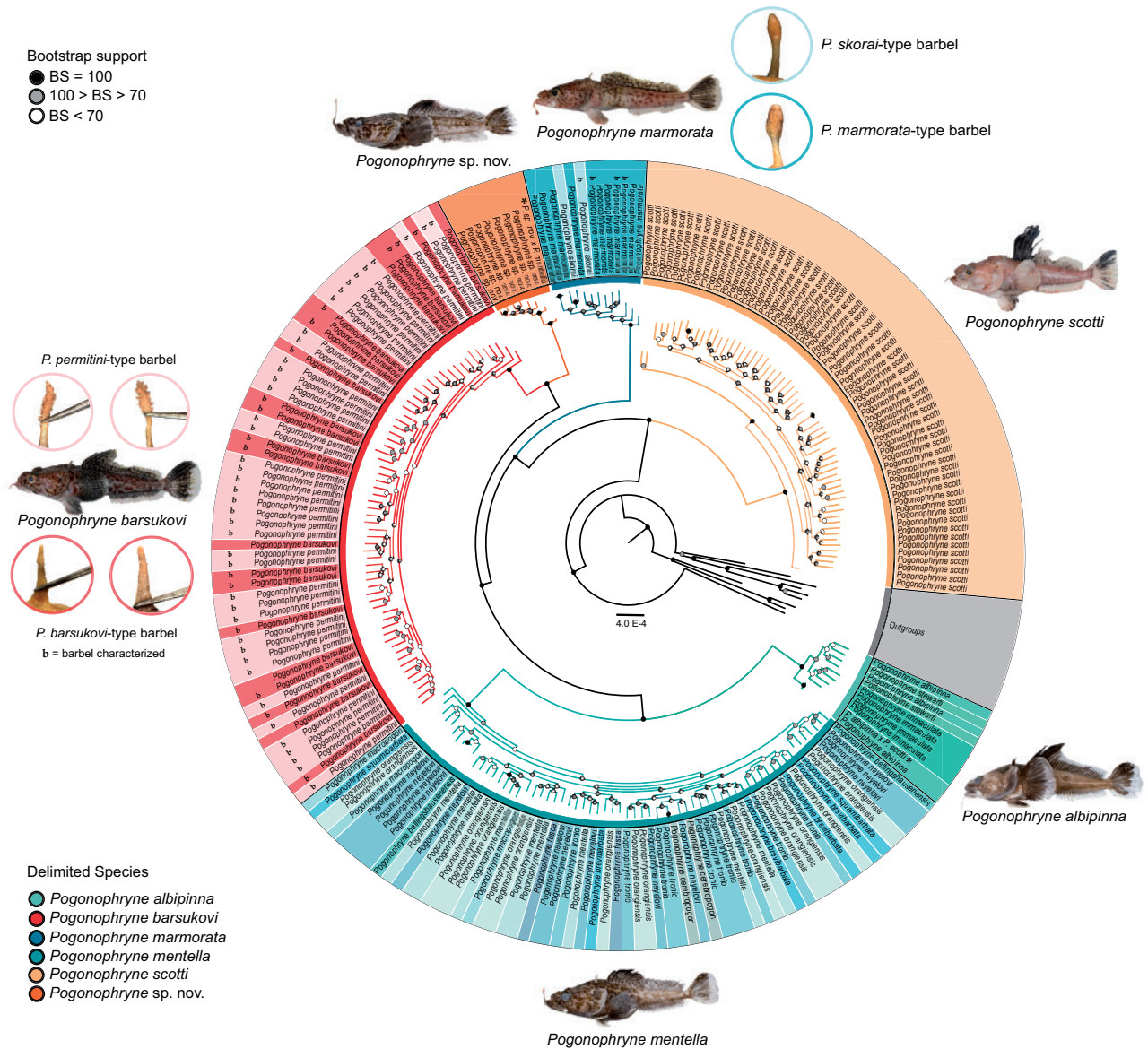
FIGURE 2.   Maximum likelihood (IQ-TREE) phylogeny of *Pogonophryne* based on analysis of 28,272 ddRAD loci (min174 data set). Shaded circles at each node indicate bootstrap support. The current delimitation of species is indicated by color shading: green = *Pogonophryne albipinna*, red = *P. barsukovi*, dark blue = *P. marmorata*, light blue = *P. mentella*, light orange = *P. scotti*, and dark orange = *Pogonophryne* sp. nov. No additional species in the clades that comprise the delimited *P. barsukovi*, *P. marmorata*, *P. albipinna*, and *P. mentella* are resolved as monophyletic. The polymorphic mental barbel morphology observed in *P. marmorata* and *P. barsukovi* are shown. Each specimen of *P. barsukovi*, "*P. permitini*," *P. marmorata*, and "*P. skorai*" scored for barbel morphology is indicated with a "b" next to the species name in the phylogeny. Peter Marriott (NIWA) provided photographs of *P. marmorata*, *P. mentella*, and *P. scotti*. (For interpretation of the references to color in this figure, the reader is referred to the web version of this article.)

in DAPC (Fig. 3a; Supplementary Fig. S4 available on Dryad). The only exceptions to these patterns of concordance between the results of STRUCTURE and DAPC involve the assignment of the two putative hybrid individuals to clusters. Specifically, the sample identified as admixed between *Pogonophryne* sp. nov. and *P. mentella* (NMNZ P.049757) using STRUCTURE was consistently identified to the *Pogonophryne* sp. nov. cluster with PP ≥ 0.99 with almost no evidence of admixed ancestry with the *P. mentella* cluster using DAPC (Fig. 3a;

Supplementary Fig. S4 available on Dryad). On the other hand, the sample identified as admixed between *P. scotti* and *P. albipinna* (NMNZ P.046208) was assigned to the *P. scotti* cluster (posterior probability = 1.0) in the DAPC analysis of the 25% complete data matrix, but was assigned to the *P. albipinna* cluster (posterior probability = 1.0) in DAPC analyses of all other data sets (Fig. 3a; Supplementary Fig. S4 available on Dryad).

Examination of genetic differentiation among the five traditionally recognized *Pogonophryne* species groups
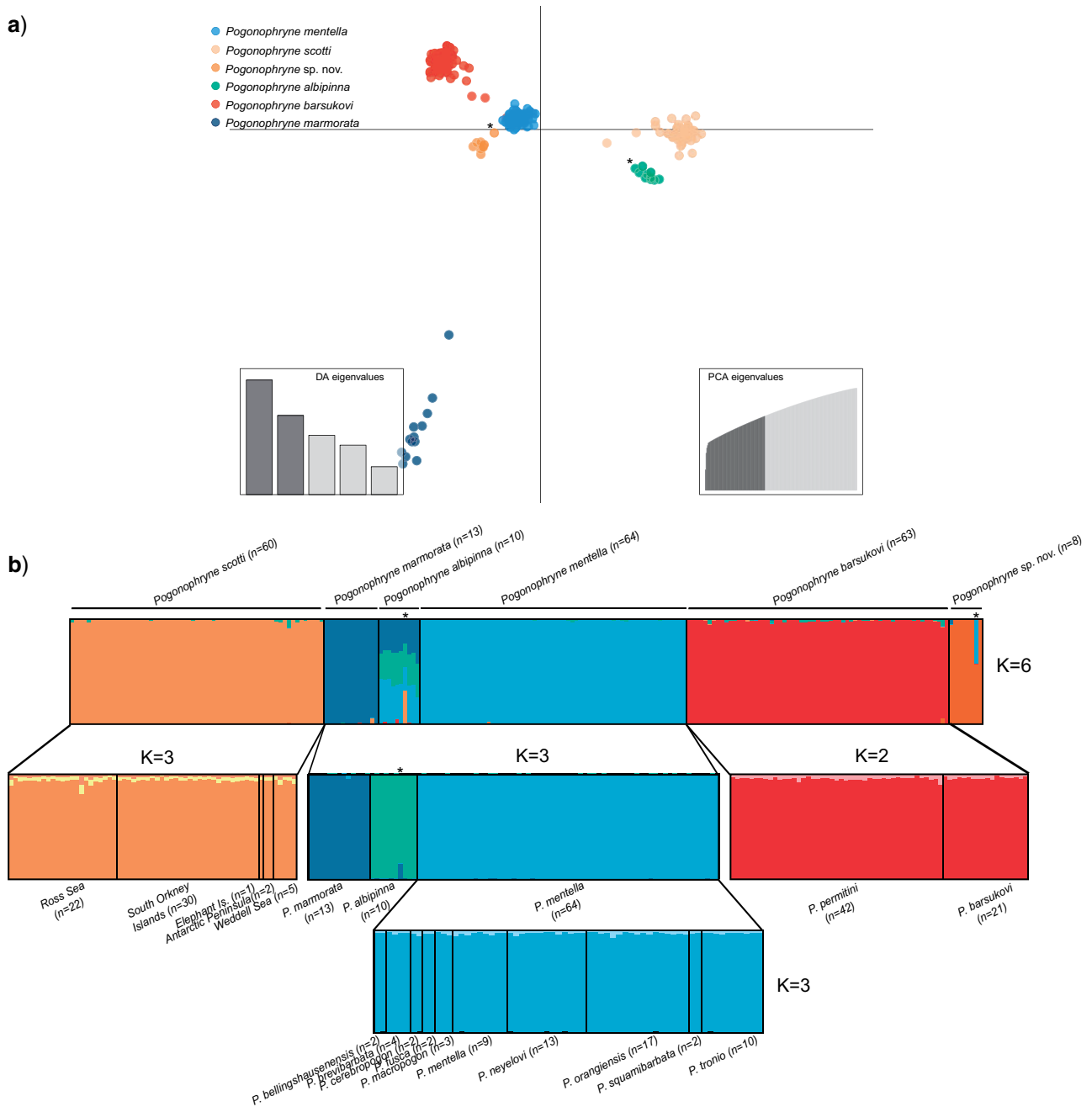
FIGURE 3.   a) Results of DAPC based on the noOut_min165 data set with 80 PC axes retained visualized as a biplot of the first two discriminant functions identified by DAPC; points represent individuals and are colored according to cluster assignment, and points indicated by asterisks represent individuals identified as putative hybrids by STRUCTURE. b) Barplot visualization of results of hierarchical Bayesian clustering analyses in STRUCTURE. Each vertical bar represents an individual, and each bar is colored according to the posterior probability of membership of that individual to a particular cluster. Asterisks indicate putative hybrids. (For interpretation of the references to color in this figure, the reader is referred to the web version of this article.)

and the putatively new species *Pogonophryne* sp. nov. revealed pairwise F_{ST} estimates reflective of strongly structured populations, ranging from 0.39 (representing the pairwise differentiation between *P. albipinna* and *P. barsukovi*) to 0.60 (pairwise differentiation between *Pogonophryne* sp. nov. and *P. marmorata*; Supplementary

Table S5 available on Dryad). However, we find little-to-no evidence of genetic differentiation between traditionally delimited species within each species group. For instance, within the *P. mentella* group, weighted F_{ST} estimates for all pairwise comparisons among the 10 traditionally delimited species range from 0 to 0.06,

indicating that groups of individuals differentiated by barbel morphology exhibit little to no genetic differentiation (Supplementary Table S5 available on Dryad). Similarly, when individuals are assigned to groups according to sampling locality, F_{ST} estimates indicate that populations spanning the Ross Sea to the Weddell Sea within both *P. barsukovi* (F_{ST} = 0–0.009) and *P. scotti* (F_{ST}: 0–0.01; Supplementary Table S5) are effectively panmictic. Estimates of Nei's genetic distance (D_{Nei}) between populations revealed very weak differentiation among traditionally recognized species groups and *Pogonophryne* sp. nov., with pairwise distances ranging from 0.02 (between *P. albipinna* and *P. mentella*) to 0.07 (between *Pogonophryne* sp. nov. and *P. marmorata*; Supplementary Table S6 available on Dryad). Within each of these groups, genetic distances among traditionally delimited species and among geographically delimited groups are generally an order of magnitude lower than those observed between species groups (Supplementary Table S6 available on Dryad).

Species Delimitation

Results of our species delimitation analyses conclusively reject hypotheses that delimit more than six species of *Pogonophryne*. BPP analyses consistently revealed support for between five and six *Pogonophryne* species depending on the prior specifications. Across all runs under a population size prior of $\theta \sim$ IG [3,0.002], nodes representing bipartitions between clades representing each of the five traditionally defined species groups and the newly discovered *Pogonophryne* sp. nov. were strongly supported (PP ≥ 0.95; Fig. 4a), yielding support for a six-species delimitation model. However, under a prior of $\theta \sim$ IG [3,0.2], the bipartition between *P. barsukovi* and *P*. sp. is not strongly supported (PP ≤ 0.95; Fig. 4a), resulting in support for a five-species model in which *P. barsukovi* and *P*. sp. nov. are lumped, but *P. scotti*, *P. marmorata*, *P. mentella*, and *P. albipinna* are distinct. Within each of these six major clades, nodes representing splits among sampled individuals consistently received low posterior support (PP <0.95; Fig. 4a) across all tests, providing no support for additional species within each of the six BPP-delimited species (PP ≤ 0.95; Fig. 4a). The only exception to this pattern is that, within the *P. albipinna* clade, the node representing the split between *Pogonophryne immaculata* and sister taxa *P. stewarti* and *P. albipinna* is strongly supported (PP ≥ 0.95; Fig. 4a) in a subset of analyses under priors $\theta \sim$ IG [3,0.002] and $\tau \sim$ IG [3,0.002].

Divergence Time Estimation

As expected from the age calibration applied to the MRCA of *Pogonophryne* in our SNAPP analysis, the divergence of *P. scotti* from all other species of *Pogonophryne* is estimated to have occurred during the Pleistocene, approximately 1 million years ago (Ma) (HPD 95% = 0.53–1.5 Ma; Fig. 5). Within *Pogonophryne* there are two sister species pairs, *P. mentella–P. albipinna* and *P. barsukovi-P*. sp. that each share common ancestry at approximately 500,000 years ago (Fig. 5).

Morphological Analyses

Visualization of the first three PC axes reveals near-complete overlap of each of the five traditionally defined species groups and the putatively new species in morphospace (Fig. 4b; Supplementary Fig. S6 available on Dryad), providing no evidence for distinction among species groups along these major axes of body shape variation. The first three PCs collectively explain 44.0% of the variation in body shape. The first PC axis (21.9% of variation) mostly represents the head length and the first and second antedorsal distances, the second PC axis (14.0%) mostly describes variation in the body depth at origin of anal fin and body depth at the origin of the second dorsal fin, and the third PC (8.1%) primarily represents variation in the length of the longest first dorsal fin spine and length of the longest second dorsal fin ray (Supplementary Fig. S6 available on Dryad). PC analyses conducted independently within each of the *P. mentella* and *P. barsukovi* species groups also revealed almost complete overlap in morphospace among the traditionally delimited species within these groups (Supplementary Fig. S7 available on Dryad). Finally, we find no evidence for significant distinctions between male and female individuals based on the size-corrected morphometric variables within any of the *Pogonophryne* species groups examined (results not shown).

However, we do find significant differences among species groups in specific meristic traits (Fig. 4c; Supplementary Fig. S8 and Tables S7 and S8 available on Dryad). *Pogonophryne scotti* exhibits a significantly lower mean number of second dorsal fin rays compared with all other species groups (25 vs. 27–28 second dorsal fin rays; pairwise rank-sum Wilcoxon test: $P < 0.05$ for all comparisons) and the *P. marmorata* group exhibits significantly fewer pectoral fin rays compared with all other species groups (18 vs. 20 pectoral fin rays, $P < 0.05$ for all comparisons; Supplementary Fig. S8 and Tables S7 and S8 available on Dryad). Furthermore, the mean number of abdominal vertebrae exhibited by the *P. mentella* group is significantly higher than that of any other species group (16 vs. 14–15 abdominal vertebrae; $P < 0.05$ for all comparisons), while *P. scotti* is characterized by a significantly lower number of caudal vertebrae compared with the other species groups (21 vs. 22–23 caudal vertebrae, $P < 0.05$ for all comparisons; Supplementary Fig. S8 and Tables S7 and S8 available on Dryad). There is no differentiation in meristic traits among the traditionally delimited species within the *P. mentella* group (Supplementary Tables S7 and S8 available on Dryad). Evaluation of differences in lower jaw length revealed that *Pogonophryne* sp. nov. exhibits a proportionally longer lower jaw (mean LJL:SL = 20.26%) compared with all other delimited species (mean
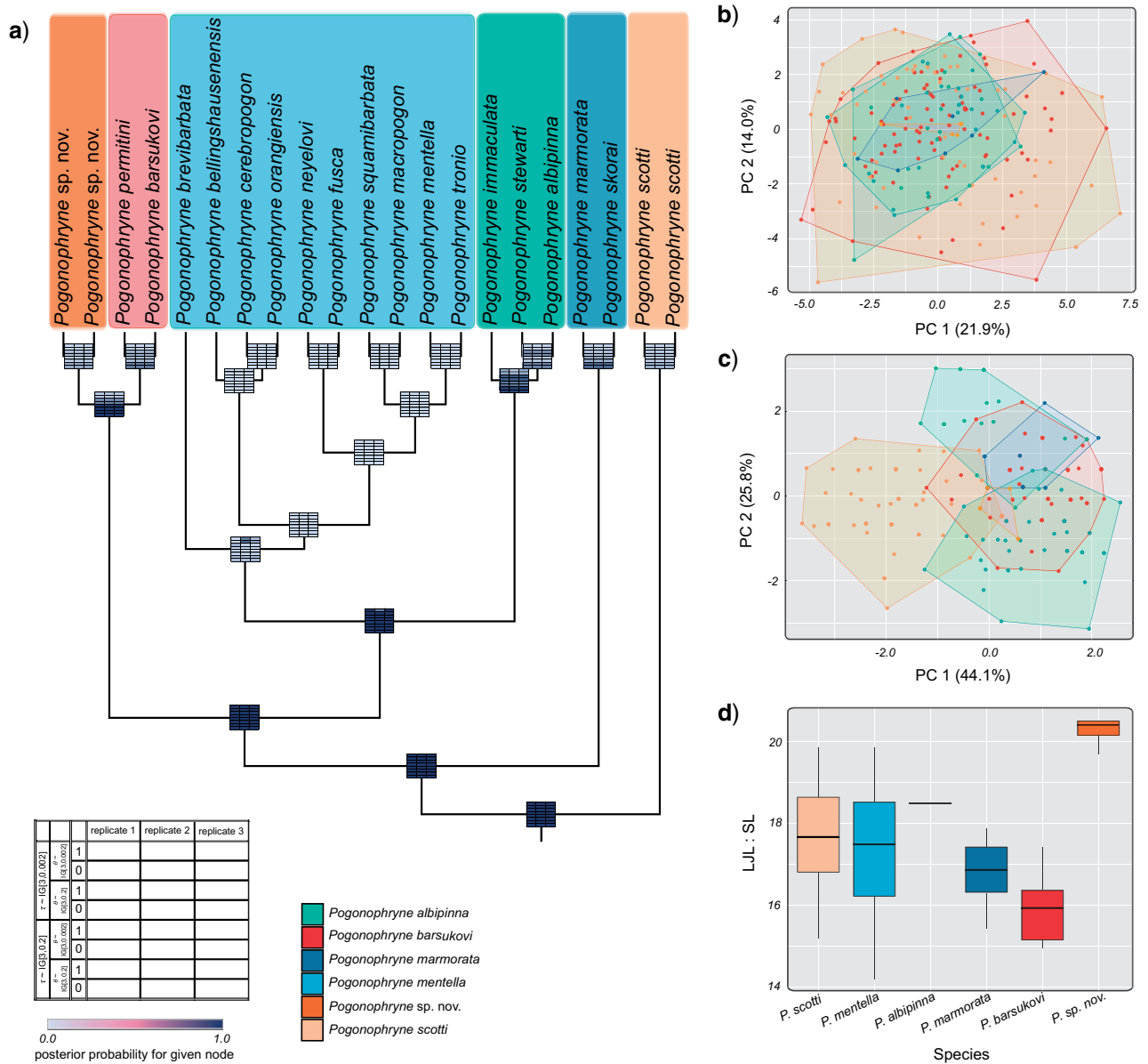
FIGURE 4. a) Results of tests of a 21-species hypothesis using a fixed guide tree for *Pogonophryne* using BPP (based on Figs. 2 and 3 from Pie et al. 2019). Heatmaps at nodes reflect posterior probabilities for the presence of that node based on BPP analyses under different species delimitation algorithms and prior settings. Tip labels in the phylogeny are placed in colored boxes that correspond to the six delimited species. b) Results of PCA of body shape variation among the six delimited species of *Pogonophryne*, visualized as a biplot of the first two PC axes. Points and convex hulls are colored according to the delimited species. c) Results of PCA of meristic trait variation among the six delimited species of *Pogonophryne*, visualized as a biplot of the first two PC axes. Points and convex hulls are colored according to the delimited species. d) Mean and standard deviation of the ratio of the length of the lower jaw and standard length (LJL:SL) for each of the six delimited species of *Pogonophryne*. (For interpretation of the references to color in this figure, the reader is referred to the web version of this article.)

LJL:SL ratios range from 15.95% to 18.49%) (Fig. 4d; Supplementary Table S9 available on Dryad).

Examination of barbel morphology in the 56 specimens identified as *P. barsukovi* or *P. permitini* resulted in 15 specimens exhibiting the "*barsukovi*" type and 41 specimens exhibiting the "*permitini*" morphology (Supplementary Table S10 available on Dryad). As

shown in Figure 2, the "*barsukovi*" barbel is short and tapered to a point and the "*permitini*" barbel has a terminal expansion with finger-like processes as described by Andriashev (1967) and Eakin (1990). Among the four specimens identified as *P. marmorata* or *P. skorai*, three exhibited the "*marmorata*" barbel that is short with a terminal expansion that is wider than
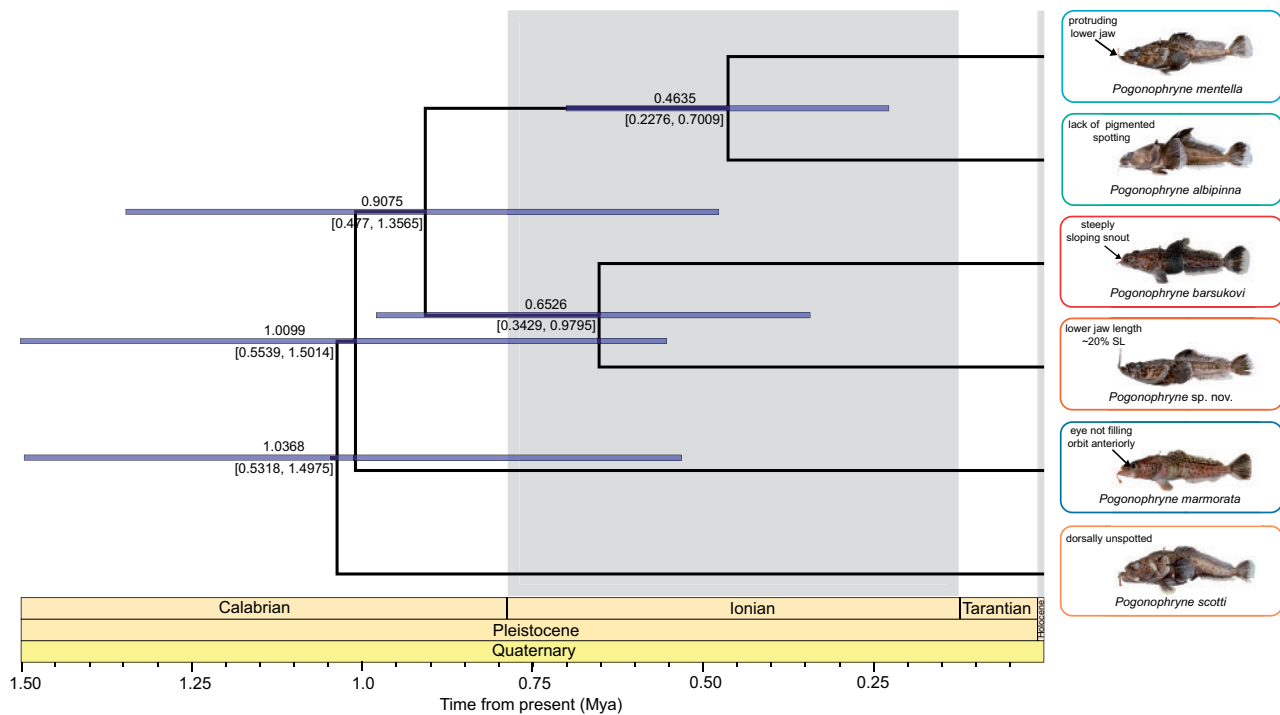
FIGURE 5. Summary of species delimitation, diagnostic morphological traits, and divergence times within *Pogonophryne*. Species tree and divergence times estimated from SNAPP for the six species delimited in this study. Node bars represent the 95% highest posterior density intervals for estimated divergence times for each node. The range of this age interval is shown numerically below the node bar, and the mean age estimate for each node is given above the bar. Peter Marriott (NIWA) provided photographs of *P. barsukovi* and *P. marmorata*. (For interpretation of the references to color in this figure, the reader is referred to the web version of this article.)

the stalk (Fig. 2; Eakin 1990). Only one of the specimens exhibited the "*skorai*" barbel morphology that has a short and less developed terminal expansion with a flattened shape (Fig. 2; Balushkin and Spodareva 2013c). In the ddRAD-inferred phylogeny, specimens exhibiting the disparate barbel morphologies that are delimited as *P. barsukovi* do not resolve as monophyletic groups and the two specimens identified as *P. skorai*, one of which is confirmed as having a barbel consistent with this identification, also do not resolve as a clade in the phylogeny (Fig. 2).

DISCUSSION

The increasing application of genomic-scale DNA sequence data and coalescent-based species delimitation protocols has not only yielded unprecedented resolution of species boundaries (Wagner et al. 2013; Gratton et al. 2016; Herrera and Shank 2016; Loureiro et al. 2020) but has facilitated the discovery of morphologically cryptic diversity in lineages spanning the tree of life (Barley et al. 2013; Feinberg et al. 2014; de Oca et al. 2017; Spriggs et al. 2019). However, combining genomic data with coalescent-based approaches for fine-scale resolution of genetic structure has the potential to misidentify

population-level differentiation as representing divergences among independently evolving species that can lead to inflated estimates of species diversity (Sukumaran and Knowles 2017; Chambers and Hillis 2020). In the face of the common expectation that genomic-based species delimitation will trend toward elevating recognized species diversity, our analyses of genomic variation in *Pogonophryne* using phylogenetic, population genetic, and coalescent-based approaches result in a dramatic reduction of the number of distinct species recognized within the clade. The results of the genomic delimitation are supported by analysis of the available morphological data, which shows near-complete overlap in multivariate space (Fig. 4b; Supplementary Fig. S6 available on Dryad). Following a unified general lineage concept of species (de Queiroz 1998, 2007), we identify evidence for six species of *Pogonophryne* that represent independently evolving metapopulation lineages. These six species of *Pogonophryne* correspond to each of the five traditionally recognized species groups (*sensu* Balushkin and Eakin 1998) and the newly discovered lineage *Pogonophryne* sp. nov. Our findings provide no evidence to support the recognition of more than six species and we propose that an additional 24 of the available 34 species names for *Pogonophryne* are synonyms of the five named species delimited in our

genomic and morphological analyses (Supplementary Table S11 available on Dryad). Although we cannot rule out the possibility that the *Pogonophryne* species unsampled in our analyses represent evolutionarily distinct lineages, we propose that the variation in barbel morphology used to distinguish these species likely lies within the range of intraspecific barbel variation that characterizes each of the species we delimit here.

An Integrative Approach to Species Delimitation

Species represent the fundamental units of analysis in ecology, evolutionary biology, and conservation; thus, accurate delimitation of species represents an important goal of systematics research. However, species delimitation remains challenging in recent, rapid species radiations, where it is difficult to distinguish population-level structure from boundaries representing divergences among incipient species. The increasing availability of genomic-scale DNA sequence data is a boon for addressing such challenges. For instance, in several recent, rapid evolutionary radiations, genetic data have provided unprecedented resolution of species boundaries that have been previously delimited on the basis of morphological, geographic, or ecological data (Wagner et al. 2013; Gratton et al. 2016; Herrera and Shank 2016; Loureiro et al. 2020). In other cases, molecular-based species delimitation studies have frequently yielded findings of more species diversity than has previously been recognized on the basis of morphology alone, particularly in nonadaptive radiations or cryptic species complexes (Barley et al. 2013; Feinberg et al. 2014; de Oca et al. 2017; Spriggs et al. 2019). Case studies in which application of molecular data has revealed evidence for fewer species than previously recognized are comparatively rare in the literature. However, our work joins the ranks of a few recent investigations in which analyses of molecular data reveal taxonomic oversplitting on the basis of morphological analyses (Kreuzinger et al. 2015; Federman et al. 2018; Hundsdoerfer et al. 2019; Ludt et al. 2019), suggesting that such a result is more common than previously realized.

Just as population-level genetic structure is difficult to unambiguously distinguish from genetically distinct species, intraspecific polymorphism in a given trait can be difficult to unambiguously distinguish from fixed character state differences between species (Wiens and Servedio 2000). Identification of fixed and/or nonoverlapping character state differences is especially challenging when the number of individuals sampled for morphology-based species delimitation is relatively small or when only a small number of phenotypic characters are evaluated (Davis and Nixon 1992). These potential challenges are highlighted by lineages spanning the Malagasy plant clade *Canarium* (Federman et al. 2018), the western Palearctic spurge hawkmoths (*Hyles euphorbiae* complex; Hundsdoerfer et al. 2019), and the tadpole barbeled plunderfishes (*Pogonophryne*;

this study). In each of these cases, relatively high proportions of species were described from a relatively small number of specimens (i.e., <10 individuals per species description) and were distinguished primarily on the basis of a single character (e.g., Hundsdoerfer et al. 2011; Balushkin and Spodareva 2015; Daly et al. 2015). However, application of molecular-based approaches to species delimitation within each of these clades revealed that consistent differences in characters such as barbel ornamentation or color pattern were often not associated with genetically distinct lineages, prompting a re-evaluation of characters once thought to be of high diagnostic importance (Federman et al. 2018; Hundsdoerfer et al. 2019).

While subtle differences in quantitative or qualitative phenotypic characters can provide evidence that populations represent independently evolving species, phenotypic variation is not always associated with genetic differentiation of populations or species (e.g., Harley et al. 2006; Kreuzinger et al. 2015). Indeed, observations of wide-ranging intraspecific variation in traits such as color patterns are not uncommon for many fish lineages (e.g., Puebla et al. 2008; Ludt et al. 2019). Thus, caution should be exercised in relying on a single character to delimit and describe species diversity, particularly when the material available for species description are limited. Our work joins the ranks of other recent case studies in demonstrating that challenges related to limited sampling may be overcome by applying an integrative approach to taxonomy and species delimitation, in which analyses of phenotypic variation are combined with genetic, ecological, and geographic data (Federman et al. 2018; Hundsdoerfer et al. 2019). Indeed, even when clades of interest are extensively sampled, the use of either morphological or molecular data alone for investigating species boundaries may yield spurious conclusions (Gratton et al. 2016; Sukumaran and Knowles 2017), and a more robust approach to species delimitation should rely on the incorporation of multiple lines of evidence.

Support for a Reduction of Recognized Species Diversity in Pogonophryne

Morphological traits identified by expert opinion have been historically heralded as a gold standard of species delimitation. However, our analyses of genomic data suggest that in the case of *Pogonophryne,* such a practice can promote dramatic taxonomic inflation. Our results provide no genomic or phenotypic support for differentiation among species of *Pogonophryne* that are diagnosed exclusively using barbel morphology. At the same time, our analyses provide evidence for the existence of a sixth deeply diverging lineage that likely represents an undescribed species of *Pogonophryne* (Figs. 2, 3, and 4a,d). Phylogenetic analyses of ddRAD data consistently resolve a clade comprising seven individuals previously identified from morphology to six different species, and the results of both STRUCTURE

and DAPC consistently assign these seven individuals to their own discrete genotypic cluster. In addition to the phylogeny and genomic clustering analyses (Figs. 2 and 3), the BPP species delimitation analysis supports the distinctiveness of the newly discovered *Pogonophryne* sp. nov. relative to its sister lineage, *P. barsukovi*, although we note that support for this distinction depends on the priors applied to the population size parameter (θ). Specifically, under a prior of θ~ IG [3,0.2], lumping of *Pogonophryne* sp. nov. with *P. barsukovi* was strongly supported (Fig. 4a). Consistent with the genomic analyses, morphological analyses reveal that a longer lower jaw length in proportion to SL diagnoses the newly discovered *Pogonophryne* sp. nov. (Fig. 4d). Additional molecular and morphological analyses are required to fully delimit and describe this newly discovered species of *Pogonophryne*.

Our findings are concordant with previous phylogenetic analyses of *Pogonophryne* based on mtDNA sequences (Eakin et al. 2009) that provided strong support for monophyly of the five traditionally recognized *Pogonophryne* species groups with no support for the genetic distinctiveness of species within each group. As such, the discordance between the 29 species recognized in the current taxonomy and the six species of *Pogonophryne* delimited here is likely due to the unreliability of mental barbel variation for species diagnosis and description (Fig. 2). The utility of the mental barbel as a diagnostic character was demonstrated as inadequate in a case study that resulted in the synonymization of *Pogonophryne dolichobranchiata* and *Pogonophryne phyllopogon* with *P. scotti* (Balushkin and Eakin 1998; Eakin et al. 2001). Similar findings of extensive intraspecific variation in barbel morphology are reported in other species of Artedidraconidae, *Artedidraco mirus* and *Dolloidraco longedorsalis* (Eastman and Eakin 2001; Eakin et al. 2006), suggesting that high variability in this trait is likely a general trend in this more inclusive clade.

The functional significance of the mental barbel in plunderfishes remains uncertain. Observations of feeding behavior in some artedidraconid species (e.g., *Histiodraco velifer*; Janssen et al. 1993) suggest that the barbel functions as both a lure and a somatosensory organ important for feeding. Meanwhile, in other species (e.g., *P. marmorata*; Iwami et al. 1996), the barbel may function as a sensor to detect prey, but not as a lure, or does not appear to function in either luring or detection of prey (e.g., *Artedidraco skottsbergi*; Iwami et al. 1996). It is therefore unclear whether intraspecific variability in the length and ornamentation of the mental barbel terminal expansion has any adaptive or functional significance (Eakin et al. 2006). Furthermore, studies of intraspecific variation in the barbel within multiple artedidraconid species generally reveal no evidence for correlations between barbel type or length and sex, body size, or geography (Eakin et al. 2001; Eastman and Eakin 2001; Eakin et al. 2006). Thus, the factors underlying the extensive intraspecific variability of the mental barbel in plunderfish species remain uncertain.

Maintenance of Species Boundaries

The six putative *Pogonophryne* species delineated in this study exhibit near-complete overlap in their geographic ranges (Fig. 1), with five of the six species exhibiting approximately circum-Antarctic distributions. Similar broad circum-Antarctic coexistences between closely related species within the cryonotothenioid radiation are often attributed to depth-related stratification of the water column and/or partitioning of feeding niches (Rutschmann et al. 2011; Near et al. 2012; Marino et al. 2013). However, this is unlikely to be the case for *Pogonophryne.* There is extensive overlap among these six lineages along the axis of depth, with only *P. albipinna* exhibiting a preference for substantially deeper habitats (884–2542 m; Eastman 2017) compared with all other *Pogonophryne* species, which range in bathymetric distributions from 80 to 1947 m (Eastman 2017). Moreover, species of *Pogonophryne* generally appear to exhibit significant niche overlap, particularly along the axes of diet (Wyanski and Targett 1981; Olaso et al. 2000; Lombarte et al. 2003), buoyancy (Near et al. 2012; Eastman 2017), and niche-identifying isotope ratios (Rutschmann et al. 2011). Studies of *Pogonophryne* feeding ecology consistently identify all examined species as benthic feeders that use a sit-and-wait approach to capture primarily amphipods, isopods, and mysids moving just above or on the shelf substrate (Wyanski and Targett 1981; Olaso et al. 2000; Lombarte et al. 2003). As such, the currently available evidence does not provide strong support for the hypothesis of ecological differentiation among sympatrically distributed species of *Pogonophryne*.

The large degree of ecological niche overlap in widespread sympatry raises the question of how boundaries among *Pogonophryne* species are maintained. On the one hand, it is possible that the coexistence of *Pogonophryne* species during interglacial periods have provided opportunities for interspecific gene flow. The identification of two potential hybrid individuals (NMNZ P.049757 and NMNZ P.046208) in our STRUCTURE analyses suggests that interspecific gene flow within *Pogonophryne* is possible and that the boundaries we observed are not discrete over time. However, the limited number of observations supporting this conclusion provide little evidence to suggest that hybridization among sympatric species is extensive, nor that it has resulted in the collapse of barriers between species. Instead, we suggest that species boundaries are likely maintained by behavioral mechanisms promoting prezygotic reproductive isolation. Observations of nest guarding behavior for *P. scotti* (Jones and Near 2012) and widespread sexual dimorphism in several *Pogonophryne* species (Eakin 1990; Jones and Near 2012) provide evidence to suggest that species-specific courtship and parental care behaviors may represent barriers to gene flow among sympatrically distributed species. This hypothesis is additionally supported by observations of similar differentiation in mating associated behaviors between closely related notothenioid species, such as nesting differences between the muddy or silty substrate utilizing

Chaenocephalus aceratus (Detrich et al. 2005), and the flat-stone utilizing *Chaenodraco wilsoni* (Ziegler et al. 2017; La Mesa et al. 2021). It is possible that such species-specific differences in nesting and courtship behaviors promote reproductive isolation among *Pogonophryne* species. Further studies regarding reproductive behaviors in *Pogonophryne* are warranted and have the potential to illuminate general mechanisms that maintain species boundaries between ecologically similar marine fishes in sympatry.

Diversification of Pogonophryne

As the number of species provide the operational units for the calculation of diversification rates (Alfaro et al. 2009; Rabosky et al. 2014), species delimitation is fundamental for accurate quantification of lineage diversification dynamics. Currently, it is hypothesized that cryonotothenioids exhibit at least two shifts to elevated rates of lineage diversification: one at the most recent common ancestor (MRCA) of all cryonotothenioids and a second at the MRCA of Artedidraconidae (Near et al. 2012; Daane et al. 2019), in which *Pogonophryne* comprises 76% of the species diversity (Eastman and Eakin 2000; Lecointre et al. 2011; Eschmeyer and Fricke 2020). However, our revised classification recognizes only six species of *Pogonophryne* which fundamentally impacts estimates of lineage diversification. Using Equation 4 in Magallón and Sanderson (2001) to calculate the rate of lineage diversification at the crown node of a clade under a birth–death model results in a rate of diversification of 2.59 species per million years (sp/Myr) if there are 29 species of *Pogonophryne* and the MRCA age is 1.4 Ma (Fig. 5). In contrast, the lineage diversification rate is reduced by more than 50% (1.06 sp/Myr) when only six species of *Pogonophryne* are delimited. This reduction in the rate of diversification provides new insights into the mode and tempo of speciation of cryonotothenioids during the Pleistocene (Fig. 5; Near et al. 2012).

The Pleistocene is characterized by frequent climatic fluctuations associated with repeated cycles of glacial advance and retreat (Huybrechts 2002; Naish et al. 2009) that are hypothesized to promote the recurrent generation of ecological opportunities for speciation and phenotypic divergence in the cryonotothenioid adaptive radiation (Rutschmann et al. 2011; Near et al. 2012; Dornburg et al. 2017; Daane et al. 2019). While ecological opportunity is often invoked as a catalyst of lineage diversification (Yoder et al. 2010; Stroud and Losos 2016), *Pogonophryne* are not disparate in terms of morphology (Fig. 4b; Supplementary Fig. S6 available on Dryad) or feeding ecology (Lombarte et al. 2003). Given this lack of ecological or phenotypic divergence, we suggest allopatric speciation in refugia during periods of glacial maxima to represent a more likely mechanism of diversification among the six living species of *Pogonophryne*. Indeed, sediment core data suggest that approximately 38 cycles of glacial advance and retreat have occurred over the last 5 million years with a periodicity of ~100,000 years (Allcock and Strugnell 2012), and it has been suggested previously that these frequent glacial cycles may have provided opportunities for the allopatric divergence of Antarctic notothenioid lineages in glacial refugia (Near et al. 2012; Dornburg et al. 2017).

Conclusions

Although Antarctic notothenioids represent a particularly well-studied example of an adaptive radiation of marine teleost fishes (Near et al. 2012; Colombo et al. 2015; Matschiner et al. 2015; Dornburg et al. 2017), our understanding of the mechanisms of lineage diversification within this radiation remains limited, due in part to uncertainty in the number of species in the clade. For example, systematists debate whether the Kerguelen Islands endemic icefish lineage *Channichthys* comprises one to nine species (Eastman and Eakin 2000; Nikolaeva and Balushkin 2019). These types of taxonomic controversies each require individual investigations. Recent genetic analyses have synonymized long recognized species (Lautredou et al. 2010; Rey et al. 2011), validated contentious species boundaries (Dornburg et al. 2016a), and led to the discovery of morphologically cryptic cryonotothenioid species (Dornburg et al. 2016b). Our analysis of species diversity in *Pogonophryne* demonstrates how the integration of genomic and morphological data sheds light both on the overestimation of species diversity and the discovery of new presumably morphologically cryptic species. A critical examination of currently recognized cryonotothenioid species boundaries represents a vital requirement for future investigations of the mechanisms driving diversification within this remarkable adaptive radiation.

Supplementary Material

Data available from the Dryad Digital Repository: http://dx.doi.org/10.5061/dryad.4f4qrfjc3. Supplemental Information available from Zenodo: https://doi.org/10.5281/zenodo.5083389. Raw sequence data are available for download from the NCBI Sequence Read Archive (SRA) (BioProject PRJNA701357).

Acknowledgments

Fieldwork was facilitated through the United States Antarctic Marine Living Resources Program and the officers and crew of the RV Yuzhmorgeologia, the

References

Alfaro M.E., Santini F., Brock C., Alamillo H., Dornburg A., Rabosky D.L., Carnevale G., Harmon L.J. 2009. Nine exceptional radiations plus high turnover explain species diversity in jawed vertebrates. PNAS. 106:13410–13414.

Allcock A.L., Strugnell J.M. 2012. Southern Ocean diversity: new paradigms from molecular ecology. Trends Eco. Evol. 27:520–528.

Andriashev A.P. 1967. Review of the plunder fishes of genus *Pogonophryne* Reagan (Harpagiferidae) with descriptions of five new species from the East Antarctic and South Orkney Islands, Pisces, Harpagiferidae. Explorations of the Fauna of the Seas IV. (XII). Biological Results of the Soviet Antarctic Expedition (1955–1958). Zool. J. Acad. Sci. U.S.S.R. 3:389–412.

Balushkin A.V. 1991. On the circumcontinental distribution of the plunderfish *Pogonophryne macropogon* Eakin (Artedidraconidae), from Antarctica. J. Ichthyol. 31:116–119.

Balushkin A.V. 1999. *Pogonophryne eakini* sp. nova (Artedidraconidae, Notothenioidei, Perciformes), a new species of the toad plunderfish from the Antarctic. J. Ichthyol. 39:799–802.

Balushkin A.V. 2013. A new species of *Pogonophryne* (Perciformes: Notothenioidei: Artedidraconidae) from the deep Ross Sea, Antarctica [in Russian]. Proc. Zool. Inst. Russ. Acad. Sci. 317:119–124.

Balushkin A.V., Eakin R.R. 1998. *Pogonophryne fusca* sp. nov. (Artedidraconidae, Notothenioidei) and notes on the species composition and groups of the genus *Pogonophryne* Regan. J. Ichthyol. 38:574–579.

Balushkin A.V., Korolkova E.D. 2013. New species of plunderfish *Pogonophryne favosa* sp. n. (Artedidraconidae, Notothenioidei, Perciformes) from the Cosmonauts Sea (Antarctica) with description in artedidraconids of unusual anatomical structures-convexitas superaxillaris. J. Ichthyol. 53:562–574.

Balushkin A.V., Petrov D., Prutko V. 2011. *Pogonophryne brevibarbata* sp. nov. (Artedidraconidae, Notothenioidei, Perciformes) – a new species of toadlike plunderfish from the Ross Sea, Antarctica. Proc. Zool. Inst. Russ. Acad. Sci. 314:381–386.

Balushkin A.V., Spodareva V.V. 2013a. Dwarf toad plunderfish *Pogonophryne minor* sp. n. (Artedidraconidae; Nototheniodei; Perciformes)—a new species and one of the smallest species of autochthonous ichthyofauna of marginal seas of the Antarctic continent. J. Ichthyol. 53:1–6.

Balushkin A.V., Spodareva V.V. 2013b. *Pogonophryne sarmentifera* sp. nov. (Artedidraconidae; Notothenioidei; Perciformes) – the deep-water species of Antarctic plunderfishes from the Ross Sea (Southern Ocean) [in Russian]. Proc. Zool. Inst. Russ. Acad. Sci. 317:275–281.

Balushkin A.V., Spodareva V.V. 2013c. *Pogonophryne skorai* sp. n. (Perciformes: Artedidraconidae), a new species of toadlike plunderfish from the Bransfield Strait and coastal waters of the south Shetland Islands, Antarctica. Russ. J. Mar. Biol. 39:190–196.

Balushkin A.V., Spodareva V.V. 2015. New species of the toad plunderfish of the "albipinna" group, genus *Pogonophryne* (Artedidraconidae) from the Ross Sea (Antarctica). J. Ichthyol. 55:757–764.

Barley A.J., White J., Diesmos A.C., Brown R.M. 2013. The challenge of species delimitation at the extremes: diversification without morphological change in Philippine sun skinks. Evolution 67(12):3556–3572.

Bernardi G., Goswami U. 1997. Molecular evidence for cryptic species among the Antarctic fish Trematomus bernacchii and Trematomus hansoni. Antarctic Sci. 9:381–385.

Bouckaert R., Vaughan T.G., Barido-Sottani J., Duchêne S., Fourment M., Gavryushkina A., Heled J., Jones G., Kühnert D., De Maio N., Matschiner M. 2019. BEAST 2.5: an advanced software platform for Bayesian evolutionary analysis. PLoS Comput. Biol. 15:e1006650.

Brandt A., Gooday A.J., Brandao S.N., Brix S., Brokeland W., Cedhagen T., Choudhury M., Cornelius N., Danis B., De Mesel I., Diaz R.J., Gillan D.C., Ebbe B., Howe J.A., Janussen D., Kaiser S., Linse K., Malyutina M., Pawlowski J., Raupach M., Vanreusel A. 2007. First insights into the biodiversity and biogeography of the Southern Ocean deep sea. Nature 447:307–311.

Brasier M.J., Wiklund H., Neal L., Jeffreys R., Linse K., Ruhl H., Glover A.G. 2016. DNA barcoding uncovers cryptic diversity in 50% of deep-sea Antarctic polychaetes. R. Soc. Open Sci. 3.

Bryant D., Bouckaert R., Felsenstein J., Rosenberg N.A., RoyChoudhury A. 2012. Inferring species trees directly from biallelic genetic markers: bypassing gene trees in a full coalescent analysis. Mol. Biol. Evol. 29:1917–1932.

Chambers E.A., Hillis D.M. 2020. The multispecies coalescent oversplits species in the case of geographically widespread taxa. Syst. Biol. 69:184–193.

Chifman J., Kubatko L. 2014. Quartet inference from SNP data under the coalescent model. Bioinformatics 30:3317–3324.

Chown S.L., Clarke A., Fraser C.I., Cary S.C., Moon K.L., McGeoch M.A. 2015. The changing form of Antarctic biodiversity. Nature 522:427–434.

Colombo M., Damerau M., Hanel R., Salzburger W., Matschiner M. 2015. Diversity and disparity through time in the adaptive radiation of Antarctic notothenioid fishes. J. Evol. Biol. 28:376–394.

Coulon A., Fitzpatrick J.W., Bowman R., Stith B.M., Makarewich C.A., Stenzler L.M., Lovette I.J. 2008. Congruent population structure

inferred from dispersal behaviour and intensive genetic surveys of the threatened Florida scrub-jay (*Aphelocoma coerulescens*). Mol. Ecol. 17:1685–1701.

Daane J.M., Dornburg A., Smits P., MacGuigan D.J., Brent Hawkins M., Near T.J., William Detrich III H., Harris M.P. 2019. Historical contingency shapes adaptive radiation in Antarctic fishes. Nat. Ecol. Evol. 3:1102–1109.

Daly D.C., Raharimampionona J., Federman S. 2015. A revision of Canarium L. (Burseraceae) in Madagascar. Adansonia, 37(2):277–345.

Danecek P., Auton A., Abecasis G., Albers C.A., Banks E., DePristo M.A., Handsaker R.E., Lunter G., Marth G.T., Sherry S.T., McVean G. 2011. The variant call format and VCFtools. Bioinformatics. 27:2156–2158.

Davis J.I., Nixon K.C. 1992. Populations, genetic variation, and the delimitation of phylogenetic species. Syst. Biol. 41(4):421–435.

de Oca A.N.M., Barley A.J., Meza-Lázaro R.N., García-Vázquez U.O., Zamora-Abrego J.G., Thomson R.C., Leaché A.D. 2017. Phylogenomics and species delimitation in the knob-scaled lizards of the genus Xenosaurus (Squamata: Xenosauridae) using ddRADseq data reveal a substantial underestimation of diversity. Mol. Phylogenet. Evol. 106:241–253.

de Queiroz K. 1998. The general lineage concept of species, species criteria, and the process of speciation: a conceptual unification and terminological recommendations. In: Howard D.J., Berlocher S.H., editors. Endless forms: species and speciation. Sunderland: Sinauer. p. 57–75.

de Queiroz K. 2007. Species concepts and species delimitation. Syst. Biol. 56:879–886.

Degnan J.H., Rosenberg N.A. 2009. Gene tree discordance, phylogenetic inference and the multispecies coalescent. Trends Ecol. Evol. 24:332–340.

Detrich H.W., Jones C.D., Kim S., North A.W., Thurber A., Vacchi M. 2005. Nesting behavior of the icefish Chaenocephalus aceratus at Bouvetøya Island, Southern Ocean. Polar Biol. 28:828–832.

Devitt T.J., Wright A.M., Cannatella D.C., Hillis D.M. 2019. Species delimitation in endangered groundwater salamanders: Implications for aquifer management and biodiversity conservation. PNAS. 116:2624–2633.

Dornburg A., Eytan R.I., Federman S., Pennington J.N., Stewart A.L., Jones C.D., Near T.J. 2016a. Molecular data support the existence of two species of the Antarctic fish genus *Cryodraco* (Channichthyidae). Polar Biol. 39:1369–1379.

Dornburg A., Federman S., Eytan R.I., Near T.J. 2016b. Cryptic species diversity in sub-Antarctic islands: a case study of *Lepidonotothen*. Mol. Phylogenet. Evol. 104:32–43.

Dornburg A., Federman S., Lamb A.D., Jones C.D., Near T.J. 2017. Cradles and museums of Antarctic teleost biodiversity. Nat. Ecol. Evol. 1:1379–1384.

Duhamel G., Hulley P.A., Causse R., Koubbi P., Vacchi M., Pruvost P., Vigetta S., Irisson J.O., Mormede S., Belchier M., Dettai, A. 2014. Biogeographic patterns of fish.

Eakin R.R. 1977. Morphology and distribution of species in the genus Pogonophryne (Pisces, Harpagiferidae). American Geophysical Union.

Eakin R.R. 1981. Two new species of *Pogonophryne* (Pisces, Harpagiferidae) from the Ross Sea, Antarctica. In: Kornicker L.S., editor. Antarcic research series, vol. 31, Biology of the Antarctic Seas IX. Washington: American Geophysical Union. p. 149–154.

Eakin R.R. 1988a. A New Species of *Pogonophryne* (Pisces, Artedidraconidae) from Queen Maud Land Antarctica. J. L. B. Smith Institute of Ichthyology Special Publication 45:1–4.

Eakin R.R. 1988b. A new species of *Pogonophryne* (Pisces: Artedidraconidae) from the South Shetland Islands, Antarctica. Proc. Biol. Soc. Wash. 101:434–437.

Eakin R.R. 1990. Artedidraconidae. In: Gon O., Heemstra P.C., editors. Fishes of the Southern Ocean. Grahamstown, South Africa: J.L.B. Smith Institute of Ichthyology. p. 332–356.

Eakin R.R., Balushkin A.V. 2000. A new species of *Pogonophryne* (Pisces: Perciformes: Artedidraconidae) from East Antarctica. Proc. Biol. Soc. Wash. 113:264–268.

Eakin R.R., Eastman J.T. 1998. New species of *Pogonophryne* (Pisces, Artedidraconidae) from the Ross Sea, Antarctica. Copeia 1998:1005–1009.

Eakin R.R., Eastman J.T., Jones C.D. 2001. Mental barbel variation in *Pogonophryne scotti* Regan (Pisces: Perciformes: Artedidraconidae). Antarctic Sci. 13:363–370.

Eakin R.R., Eastman J.T., Matallanas J. 2008. New species of *Pogonophryne* (Pisces, Artedidraconidae) from the Bellingshausen Sea, Antarctica. Polar Biol. 31:1175–1179.

Eakin R.R., Eastman J.T., Near T.J. 2009. A new species and a molecular phylogenetic analysis of the Antarctic fish genus *Pogonophryne* (Notothenioidei: Artedidraconidae). Copeia 2009:705–713.

Eakin R.R., Eastman J.T., Vacchi M. 2006. Sexual dimorphism and mental barbel structure in the South Georgia plunderfish *Artedidraco mirus* (Perciformes: Notothenioidei: Artedidraconidae). Polar Biol. 30:45–52.

Eakin R.R., Kock K.-H. 1984. Fishes of the genus *Pogonophryne* (Pisces, Harpagiferidae) collected during cruises of the Fedeal Republic of Germany (1975–1981) in West Antarctica and in the Weddell Sea. Archive FischWissenshaft 35:17–42.

Eakin R.R., Riginella E., La Mesa M. 2015. A new species of Artedidraco (Pisces: Artedidraconidae) from the Weddell Sea, Antarctica. Polar Biol. 38:1597–1603.

Eastman J.T. 2005. The nature of the diversity of Antarctic fishes. Polar Biol. 28:93–107.

Eastman J.T., Eakin R.R. 2000. An updated species list of notothenioid fish (Perciformes; Notothenioidei), with comments on Antarctic species. Arch. Fish. Mar. Res. 48:11–20.

Eastman J.T., Eakin R.R. 2001. Mental barbel and meristic variation in the Antarctic notothenioid fish *Dolloidraco longedorsalis* (Perciformes: Artedidraconidae) from the Ross Sea. Polar Biol. 24:729–734.

Eastman J.T. 2017. Bathymetric distributions of notothenioid fishes. Polar Biol. 40:2077–2095.

Eaton D., Overcast I. ipyrad: interactive assembly and analysis of RAD-seq data sets. Available from: https://github.com/dereneaton/ipyrad.

Edgar R.C. 2004. MUSCLE: a multiple sequence alignment method with reduced time and space complexity. BMC Bioinformatics 5:1–19.

Edwards D.L., Knowles L.L. 2014. Species detection and individual assignment in species delimitation: can integrative data increase efficacy? Proc. R. Soc. B 281.

Eschmeyer W.N., Fricke R. (eds) 2020. Catalog of Fishes electronic version (15 September 2020). Available from: http://research.calacademy.org/research/ichthyology/catalog/fishcatmain.asp. California Academy of Sciences, San Francisco.

Evanno G., Regnaut S., Goudet J. 2005. Detecting the number of clusters of individuals using the software structure: a simulation study. Mol. Ecol. 14:2611–2620.

Falush D., Stephens M. and Pritchard J.K. 2007. Inference of population structure using multilocus genotype data: dominant markers and null alleles. Mol. Ecol. Notes. 7:574–578.

Federman S., Donoghue M.J., Daly D.C., Eaton D.A. 2018. Reconciling species diversity in a tropical plant clade (Canarium, Burseraceae). PLoS One 13(6):e0198882.

Feinberg J.A., Newman C.E., Watkins-Colwell G.J., Schlesinger M.D., Zarate B., Curry B.R., Shaffer H.B., Burger J. 2014. Cryptic diversity in metropolis: confirmation of a new leopard frog species (Anura: Ranidae) from New York City and surrounding Atlantic coast regions. PLoS One 9(10):e108213

Galili T. 2015. dendextend: an R package for visualizing, adjusting and comparing trees of hierarchical clustering. Bioinformatics. 31:3718–3720.

Gratton P., Trucchi E., Trasatti A., Riccarducci G., Marta S., Allegrucci G., Cesaroni D., Sbordoni V. 2016. Testing classical species properties with contemporary data: how "bad species" in the brassy ringlets (Erebia tyndarus complex, Lepidoptera) turned good. Syst. Biol. 65:292–303.

Harley C.D.G., Pankey M.S., Wares J.P., Grosberg R.K., Wonham M.J. 2006. Color polymorphism and genetic structure in the sea star Pisaster ochraceus. Biol. Bull. 211(3):248–262.

Herrera S., Shank T.M. 2016. RAD sequencing enables unprecedented phylogenetic resolution and objective species delimitation in recalcitrant divergent taxa. Mol. Phylogenet. Evol. 100:70–79.

Hoang D.T., Chernomor O., von Haeseler A., Minh B.Q., Vinh L.S. 2018. UFBoot2: improving the ultrafast bootstrap approximation. Mol. Biol. Evol. 35:518–522.

Huang H., Knowles L.L. 2016. Unforeseen consequences of excluding missing data from next-generation sequences: simulation study of RAD sequences. Syst. Biol. 65:357–365.

Hundsdoerfer A.K., Mende M.B., Kitching I.J., Cordellier M. 2011. Taxonomy, phylogeography and climate relations of the Western Palaearctic spurge hawkmoth (Lepidoptera, Sphingidae, Macroglossinae). Zool. Scr. 40(4):403–417.

Hundsdoerfer A.K., Lee K.M., Kitching I.J., Mutanen M. 2019. Genome-wide SNP data reveal an overestimation of species diversity in a group of hawkmoths. Genome Biol. Evol. 11(8):2136–2150.

Huybrechts P. 2002. Sea-level changes at the LGM from ice-dynamic reconstructions of the Greenland and Antarctic ice sheets during the glacial cycles. Quatern. Sci. Rev. 21:203–231.

Iwami T., Numanami H., Naito Y. 1996. Behaviorof three species of the familyArtedidraconidae (Pisces, Notothenioidei), with reference to feeding. 17th Symposium on Polar Biology. p. 225–230.

Jakobsson M., Rosenberg N.A. 2007. CLUMPP: a cluster matching and permutation program for dealing with label switching and multimodality in analysis of population structure. Bioinformatics 23:1801–1806.

Janssen J., Jones W., Slattery M. 1993. Locomotion and feeding responses to mechanical stimuli in Histiodraco velifer (Artedidraconidae). Copeia. 3:885–889.

Ješovnik A.N.A., Sosa-Calvo J., Lloyd M.W., Branstetter M.G., Fernández F., Schultz T.R. 2017. Phylogenomic species delimitation and host-symbiont coevolution in the fungus-farming ant genus *Sericomyrmex* Mayr (Hymenoptera: Formicidae): ultraconserved elements (UCEs) resolve a recent radiation. Syst. Entomol. 42:523–542.

Jombart T., Ahmed I. 2011. adegenet 1.3–1: new tools for the analysis of genome-wide SNP data. Bioinformatics 27:3070–3071.

Jones C.D., Near T.J. 2012. The reproductive behaviour of *Pogonophryne scotti* confirms widespread egg-guarding parental care among Antarctic notothenioids.J. Fish Biol. 80:2629–2635.

Kalyaanamoorthy, S., B. Q. Minh, T. K. F. Wong, A. von Haeseler, and L. S. Jermiin. 2017. ModelFinder: fast model selection for accurate phylogenetic estimates. Nat. Methods 14:587–589.

Kamvar Z.N., Tabima J.F., Grünwald N.J. 2014. Poppr: an R package for genetic analysis of populations with clonal, partially clonal, and/or sexual reproduction. PeerJ. 2:e281.

Kamvar Z.N., Brooks J.C., Grünwald N.J. 2015. Novel R tools for analysis of genome-wide population genetic data with emphasis on clonality. Front. Genet. 6:208.

Kolde R. 2018. pheatmap: Pretty Heatmaps. R package version 1.0.10. Available from: https://CRAN.R-project.org/package=pheatmap.

Kornilios P., Thanou E., Lymberakis P., Ilgaz Ç., Kumlutaş Y., Leaché A. 2020. A phylogenomic resolution for the taxonomy of Aegean green lizards. Zool. Scr. 49:14–27.

Kreuzinger A.J., Fiedler K., Letsch H., Grill A., 2015. Tracing the radiation of Maniola (Nymphalidae) butterflies: new insights from phylogeography hint at one single incompletely differentiated species complex. Ecol. Evol 5(1):46–58.

La Mesa M., Llompart F., Riginella E., Eastman J.T. 2021. Parental care and reproductive strategies in notothenioid fishes. Fish Fish. 22:356–376.

La Mesa M., Vacchi M., Iwami T., Eastman J.T. 2002. Taxonomic studies of the Antarctic icefish genus *Cryodraco* Dollo, 1900 (Notothenioidei: Channichthyidae). Polar Biol. 25:384–390.

Lautredou A.C., Bonillo C., Denys G., Cruaud C., Ozouf-Costaz C., Lecointre G., Dettai A. 2010. Molecular taxonomy and identification within the Antarctic genus *Trematomus* (Notothenioidei, Teleostei): how valuable is barcoding with COI? Polar Sci. 4:333–352.

Lautredou A.C., Hinsinger D.D., Gallut C., Cheng C.H.C, Berkani M., Ozouf-Costaz C., Cruaud C., Lecointre G., Dettai A. 2012. Phylogenetic footprints of an Antarctic radiation: the Trematominae (Notothenioidei, Teleostei). Mol. Phylogenet. Evol. 65:87–101.

Lecointre G., Gallut C., Bonillo C., Couloux A., Ozouf-Costaz C., Dettai A. 2011. The Antarctic fish genus *Artedidraco* is paraphyletic (Teleostei, Notothenioidei, Artedidraconidae). Polar Biol. 34:1135–1145.

Lombarte A., Olaso I., Bozzano A. 2003. Ecomorphological trends in the Artedidraconidae (Pisces: Perciformes: Notothenioidei) of the Weddell Sea. Antarctic Sci. 15:211–218.

Loureiro L.O., Engstrom M.D., Lim B.K. 2020. Single nucleotide polymorphisms (SNPs) provide unprecedented resolution of species boundaries, phylogenetic relationships, and genetic diversity in the mastiff bats (Molossus). Mol. Phylogenet. Evol. 143:106690.

Ludt W.B., Bernal M.A., Kenworthy E., Salas E., Chakrabarty P. 2019. Genomic, ecological, and morphological approaches to investigating species limits: a case study in modern taxonomy from Tropical Eastern Pacific surgeonfishes. Ecol. Evol. 9(7):4001–4012.

Magallón S., Sanderson M.J. 2001. Absolute diversification rates in angiosperm clades. Evolution 55:1762–1780.

Marino I.A.M., Benazzo A., Agostini C., Mezzavilla M., Hoban S.M., Patarnello T., Zane L., Bertorelle G. 2013. Evidence for past and present hybridization in three Antarctic icefish species provides new perspectives on an evolutionary radiation. Mol. Ecol. 22:5148–5161.

Mason N.A., Fletcher N.K., Gill B.A., Funk W.C., Zamudio K.R. 2020. Coalescent-based species delimitation is sensitive to geographic sampling and isolation by distance. Syst. Biodivers. 18:269–280.

Mastretta-Yanes A., Arrigo N., Alvarez N., Jorgensen T.H., Piñero D., Emerson B.C. 2015. Restriction site-associated DNA sequencing, genotyping error estimation and de novo assembly optimization for population genetic inference. Mol. Ecol. Resour. 15:28–41.

Matschiner M., Colombo M., Damerau M., Ceballos S., Hanel R., Salzburger W. 2015. The adaptive radiation of notothenioid fishes in the waters of Antarctica. In: Riesch R., Tobler M., Plath M., editors. Extremophile fishes: ecology, evolution, and physiology of teleosts in extreme environments. Cham: Springer International Publishing. p. 35–57.

McCartney-Melstad E., Gidiş M., Shaffer H.B. 2019. An empirical pipeline for choosing the optimal clustering threshold in RADseq studies.Mol. Ecol. Resour.19:1195–1204.

Minh B.Q., Nguyen M.A.T., von Haeseler A. 2013. Ultrafast approximation for phylogenetic bootstrap. Mol. Biol. Evol. 30:1188–1195.

Musher L.J., Cracraft J. 2018. Phylogenomics and species delimitation of a complex radiation of Neotropical suboscine birds (*Pachyramphus*). Mol. Phylogenet. Evol. 118:204–221.

Naish T., Powell R., Levy R., Wilson G., Scherer R., Talarico F., Krissek L., Niessen F., Pompilio M., Wilson T., Carter L., DeConto R., Huybers P., McKay R., Pollard D., Ross J., Winter D., Barrett P., Browne G., Cody R., Cowan E., Crampton J., Dunbar G., Dunbar N., Florindo F., Gebhardt C., Graham I., Hannah M., Hansaraj D., Harwood D., Helling D., Henrys S., Hinnov L., Kuhn G., Kyle P., Laufer A., Maffioli P., Magens D., Mandernack K., McIntosh W., Millan C., Morin R., Ohneiser C., Paulsen T., Persico D., Raine I., Reed J., Riesselman C., Sagnotti L., Schmitt D., Sjunneskog C., Strong P., Taviani M., Vogel S., Wilch T., Williams T. 2009. Obliquity-paced Pliocene West Antarctic ice sheet oscillations. Nature 458:322-U84.

Nakayama Y., Yamaguchi H., Einaga N., Esumi M. 2016. Pitfalls of DNA quantification using DNA-binding fluorescent dyes and suggested solutions. PLoS One 11(3):e0150528.

Near T.J., Dornburg A., Kuhn K.L., Eastman J.T., Pennington J.N., Patarnello T., Zane L., Fernandez D.A., Jones C.D. 2012. Ancient climate change, antifreeze, and the evolutionary diversification of Antarctic fishes. Proc. Nat. Acad. Sci. USA 109:3434–3439.

Near T.J., Dornburg A., Harrington R.C., Oliveira C., Pietsch T.W., Thacker C.E., Satoh T.P., Katayama E., Wainwright P.C., Eastman J.T., Beaulieu J.M. 2015. Identification of the notothenioid sister lineage illuminates the biogeographic history of an Antarctic adaptive radiation. BMC Evol. Biol. 15:1–14.

Nguyen L.T., Schmidt H.A., von Haeseler A., Minh B.Q. 2015. IQ-TREE: a fast and effective stochastic algorithm for estimating maximum likelihood phylogenies. Mol. Biol. Evol. 32:268–274.

Nikolaeva E.A., Balushkin A.V. 2019. Morphological characteristics of Sailfish Pike *Channichthys velifer* (Channichthyidae) from the Kerguelen Islands (Southern Ocean). J. Ichthyol. 59:834–842.

Olave M., Solà E., Knowles L.L. 2014. Upstream analyses create problems with DNA-based species delimitation. Syst. Biol. 63:263–271.

Olaso I., Rauschert M., De Broyer C. 2000. Trophic ecology of the family Artedidraconidae (Pisces: Osteichthyes) and its impact on the eastern Weddell Sea benthic system. Mar. Ecol. Prog. Ser. 194:143–158.

O'Leary S.J., Puritz J.B., Willis S.C., Hollenbeck C.M., Portnoy D.S. 2018. These aren't the loci you're looking for: Principles of effective SNP filtering for molecular ecologists. Mol. Ecol. 27:3193–3206.

Pante E., Puillandre N., Viricel A.E., Arnaud-Haond S., Aurelle D., Castelin M., Chenuil A., Destombe C., Forcioli D., Valero M., Viard F., Samadi S. 2015. Species are hypotheses: avoid connectivity assessments based on pillars of sand. Mol. Ecol. 24:525–544.

Pie M.R., Bornschein M.R., Ribeiro L.F., Faircloth B.C., McCormack J.E. 2019. Phylogenomic species delimitation in microendemic frogs of the Brazilian Atlantic Forest. Mol. Phylogenet. Evol. 141:106627.

Pritchard, J. K., M. Stephens, and P. Donnelly. 2000. Inference of population structure using multilocus genotype data. Genetics 155:945–959.

Peterson B.K., Weber J.N., Kay E.H., Fisher H.S., Hoekstra H.E. 2012. Double digest RADseq: an inexpensive method for de novo SNP discovery and genotyping in model and non-model species. PloS one. 7:e37135.

Potter S. 2018. grImport2: Importing 'SVG' Graphics. R package version 0.1-4. Available from: https://CRAN.R-project.org/package=grImport2.

Puebla O., Bermingham E., Guichard F. 2008. Population genetic analyses of Hypoplectrus coral reef fishes provide evidence that local processes are operating during the early stages of marine adaptive radiations. Mol. Ecol. 17(6):1405–1415.

Rabosky D.L., Grundler M., Anderson C., Title P., Shi J.J., Brown J.W., Huang H., Larson J.G. 2014. BAMM tools: an R package for the analysis of evolutionary dynamics on phylogenetic trees. Methods Ecol. Evol. 5:701–707.

Rambaut A., Drummond A.J., Xie D., Baele G., Suchard M.A. 2018. Posterior summarization in Bayesian phylogenetics using Tracer 1.7. Syst. Biol. 67:901.

Regan C.T. 1914. Diagnoses of new marine fishes collected by the British Antarctic ('Terra Nova') expedition. Ann. Mag. Nat. Hist. (Series 8) 13(73):11–17.

Rey O., Bonillo C., Gallut C., Cruaud C., Dettai A., Ozouf-Costaz C., Lecointre G. 2011. Naked dragonfishes *Gymnodraco acuticeps* and *G. victori* (Bathydraconidae, Notothenioidei) off Terre Adelie are a single species. Cybium 35:111–119.

Rissler L.J., Apodaca J.J. 2007. Adding more ecology into species delimitation: ecological niche models and phylogeography help define cryptic species in the black salamander (*Aneides flavipunctatus*). Syst. Biol. 56:924–942.

Rosenberg N.A. 2004. DISTRUCT: a program for the graphical display of population structure. Mol. Ecol. Notes. 4:137–138.

Rutschmann S., Matschiner M., Damerau M., Muschick M., Lehmann M.F., Hanel R., Salzburger W. 2011. Parallel ecological diversification in Antarctic notothenioid fishes as evidence for adaptive radiation. Mol. Ecol. 20:4707–4721.

Sabaj M.H. 2016. Standard symbolic codes for institutional resource collections in herpetology and ichthyology: an online reference. Version 6.5 (16 August 2016). Electronically accessible at http://www.asih.org/, American Society of Ichthyologists and Herpetologists, Washington, DC.

Shandikov G.A., Eakin R.R. 2013. *Pogonophryne neyelovi*, a new species of Antarctic short-barbeled plunderfish (Perciformes, Notothenioidei, Artedidraconidae) from the deep Ross Sea. Zookeys 59–77.

Shandikov G.A., Eakin R.R., Usachev S. 2013. *Pogonophryne tronio*, a new species of Antarctic short-barbeled plunderfish (Perciformes: Notothenioidei: Artedidraconidae) from the deep Ross Sea with new data on Pogonophryne brevibarbata. Polar Biol. 36:273–289.

Smith P.J., Steinke D., Dettai A., McMillan P., Welsford D., Stewart A., Ward R.D. 2012. DNA barcodes and species identifications in Ross Sea and Southern Ocean fishes. Polar Biol. 35:1297–1310.

Snir S., Rao S. 2012. Quartet MaxCut: a fast algorithm for amalgamating quartet trees. Mol. Phylogenet. Evol. 62:1–8.

Solís-Lemus C., Knowles L.L., Ane C. 2015. Bayesian species delimitation combining multiple genes and traits in a unified framework. Evolution 69:492–507.

Spodareva V.V., Balushkin A.V. 2014. Description of a new species of plunderfish of genus *Pogonophryne* (Perciformes: Artedidraconidae) from the Bransfield Strait (Antarctica) with a key for the identification of species of the group "marmorata". J. Ichthyol. 54:1–6.

Spriggs E.L., Eaton D.A., Sweeney P.W., Schlutius C., Edwards E.J., Donoghue M.J. 2019. Restriction-site-associated DNA sequencing reveals a cryptic Viburnum species on the North American coastal plain. Syst. Biol. 68(2):187–203.

Stange M., Sánchez-Villagra M.R., Salzburger W., Matschiner M. 2018. Bayesian divergence-time estimation with genome-wide single-nucleotide polymorphism data of Sea Catfishes (Ariidae) supports miocene closure of the Panamanian Isthmus. Syst. Biol. 67:681–699.

Stroud J.T., Losos J.B. 2016. Ecological opportunity and adaptive radiation. Annu. Rev. Ecol. Evol. Syst. 47:507–532.

Sukumaran J., Knowles L.L. 2017. Multispecies coalescent delimits structure, not species. Proc. Natl. Acad. Sci. USA 114:1607–1612.

Wagner C.E., Keller I., Wittwer S., Selz O.M., Mwaiko S., Greuter L., Sivasundar A., Seehausen O. 2013. Genome-wide RAD sequence data provide unprecedented resolution of species boundaries and relationships in the Lake Victoria cichlid adaptive radiation. Mol. Ecol. 22:787–798.

Weir B.S., Cockerham C.C. 1984. Estimating F-statistics for the analysis of population structure. Evolution 1358–1370.

Wiens J.J., Servedio M.R. 2000. Species delimitation in systematics: inferring diagnostic differences between species. Proc. R. Soc. Lond. B 267(1444):631–636.

Wilson N.G., Schrodl M., Halanych K.M. 2009. Ocean barriers and glaciation: evidence for explosive radiation of mitochondrial lineages in the Antarctic sea slug Doris kerguelenensis (Mollusca, Nudibranchia). Mol. Ecol. 18:965–984.

Yang Z. 2015. The BPP program for species tree estimation and species delimitation. Curr. Zool. 61:854–865.

Yang Z.H., Rannala B. 2010. Bayesian species delimitation using multilocus sequence data. Proc. Natl. Acad. Sci. USA 107:9264–9269.

Yang Z.H., Rannala B. 2014. Unguided species delimitation using DNA sequence data from multiple loci. Mol. Biol. Evol. 31:3125–3135.

Wyanski D.M., Targett T.E. 1981. Feeding biology of fishes in the endemic Antarctic Harpagiferidae. Copeia. 686–693.

Yoder J.B., Clancey E., Des Roches S., Eastman J.M., Gentry L., Godsoe W., Hagey T.J., Jochimsen D., Oswald B.P., Robertson J., Sarver B.A. 2010. Ecological opportunity and the origin of adaptive radiations. J. Evol. Biol. 23(8):1581–1596.

Zheng X., Levine D., Shen J., Gogarten S.M., Laurie C., Weir B.S. 2012. A high-performance computing toolset for relatedness and principal component analysis of SNP data. Bioinformatics. 28:3326–3328.

Ziegler A.F., Smith C.R., Edwards K.F., Vernet M. 2017. Glacial dropstones: Islands enhancing seafloor species richness of benthic megafauna in West Antarctic Peninsula fjords. Mar. Ecol. Prog. Ser. 583:1–14.